Green Synthesis, Biological Activity and Molecular Docking Studies of Schiff Bases

A. Saritha[a*], E.V.L. Madhuri[a], K.S. Karuna[a] and S. Sree Kanth[b]
[a]St. Francis College for Women, Begumpet, Hyderabad, Telangana, India - 500016
[b]Telangana Mahila Viswavidyalayam, Koti, Hyderabad, Telangana, India - 500095

Abstract

1-butyl-3-methylimidazolium bromide mediated synthesis of eleven Schiff base compounds (**1-11**) bearing benzhydrazide moiety is carried out followed by their structural investigation based on ESI-Mass, UV-Vis, FTIR and ^{1}H NMR spectroscopic techniques. The antibacterial activity of the compounds was assessed against *Bacillus licheniformis*, *Staphylococcus epidermidis*, *Pseudomonas syringae* and *Klebsiella pneumoniae*. The DPPH assay was followed to check the antioxidant potential while BSA denaturation model was used to find the anti-inflammatory potency of the compounds. The Schiff bases are found to possess very good biological activities. Docking studies have also been conducted to understand the interaction between the ligands and the protein involved in antibacterial activity.

Key words: 1.Schiff base, 2.Ionic liquid, 3.Biological activities, 4.Docking.

1. Introduction:

The diverse biological uses of Schiff base compounds attracted a lot of research. In Schiff bases, the imine or azomethine group [-HC=N-] plays a unique role in producing these compounds with a broad range of biological activities. Numerous physiological activities, including anti-inflammatory, antibacterial, antioxidant, antiproliferative, antifungal, antipyretic and antiviral effects, are displayed by them[1-5].

Green synthetic techniques for the synthesis of Schiff bases offer sustainable and ecologically acceptable strategies. Conventional techniques use severe environments, like high temperatures and catalysts that are acidic or basic, which also produce hazardous byproducts. Green techniques, on the other hand, use softer conditions and renewable resources to create Schiff bases[6]. Microwave irradiation, ball milling, photocatalysis, hydrothermal synthesis, sonochemical synthesis, magnetic field aided synthesis and the use of cleaner solvents including water and ionic liquids are a few examples of green synthetic techniques[7].

Ionic liquids (ILs) are inorganic or organic anions combined with large and asymmetric organic cations. ILs provide unique physicochemical and solvation properties that help to produce interesting results when compared to traditional molecular solvents. As green solvents, they help in saving time and energy by enhancing the reaction kinetics. As a result, they are regarded as a successful substitute for traditional media in chemical processes, a new generation of solvents for catalysis and environmentally acceptable reaction media for organic synthesis[8].

Owing to their biological applications, eleven Schiff bases have been synthesised by condensation of furfural, indole-3-carboxaldehyde, o-Vanillin and pyridoxal with substituted benzhydrazides, following conventional and green procedures. Reaction times and yields are compared and all the compounds were tested for antibacterial, anti-inflammatory and antioxidant properties. The compounds were also subjected to docking studies and the dock scores are presented.

2. Experimental

2.1. Materials:

o-Vanillin, Pyridoxal hydrochloride, Indole-3-carboxaldehyde, Furfural, 2-hydroxybenzhydrazide, 4-Chlorobenzhydrazide, 4-Bromobenzhydrazide, 3-Nitrobenzhydrazide, 4-Nitrobenzhydrazide, DPPH, Diclofenac sodium and 1-butyl-3-methylimidazolium bromide were procured from Sigma Aldrich. Ascorbic acid and Bovine serum albumin were purchased from Himedia. The other chemicals, reagents and solvents used were of AR grade and used directly without further purification.

2.2. Physical measurements:

Mass spectra were recorded on a Agilent G6160 A infinity lab LC/MSD/IQ spectrometer. FT-IR (Fourier Transform Infrared) spectra were recorded with Bruker, Alpha ATR Spectrometer (KBr, 4000-500 cm^{-1}). Electronic spectra were recorded using Systronics UV-Vis Double beam spectrophotometer 2201.^{1}H NMR spectra were recorded with a Varian 400 MR spectrometer in DMSO d_6.

2.3. Green synthesis of Schiff bases:

The amine (10.0 mmol) and 1-butyl-3 methylimidazolium bromide (1.0 mmol) were mixed in 10 mL of ethanol and stirred to get a clear solution. Aromatic aldehyde (10.0 mmol) dissolved in 5 mL of alcohol was slowly added to the above clear solution. The resultant mixture was refluxed for the necessary amount of time till the completion of the reaction. The progress of the reaction was checked by TLC. Later, the reaction mixture was left to stand overnight for slow precipitation. The solid obtained was filtered and washed several times with ethanol, dried and recrystallized (scheme 1). The products were thereafter examined by ESI-Mass, ^{1}H NMR, UV-Vis and IR spectra. After the completion of the reaction, the ionic liquid was regenerated and utilised for three

subsequent reactions as reported[9]. Parallelly, the syntheses were also done in the absence of the ionic liquid. The reaction times and yields are compared (Table 1).

Scheme 1: Synthesis of Schiff bases

Ar

1	2	3 to 7	8 to 11
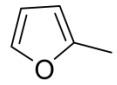	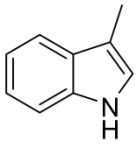	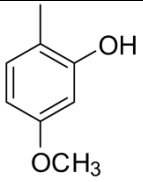	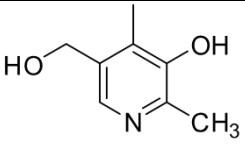

R

1, 2, 5	3, 8	4, 9	6, 10	7,11
2-OH	4-Br	4-Cl	3-NO_2	4-NO_2

Furfural-2-hydroxybenzhydrazone (1)

Pale yellow. MF, $C_{12}H_{11}N_2O_3$. mp, 172-174°C. MS, m/z: 231 [M]+. IR, ν, cm^{-1}: 3394 (O-H), 3250 (N-H), 1631 (C=O), 1604 (C=N). 1H NMR, δ, ppm: 11.80 (1H, s, N-H), 11.80 (1H, s, O-H), 8.37 (1H, s, HC=N), 7.87 (2H, d, Ar-H), 7.44 (1H, t, Ar-H), 6.96-6.97 (3H, m, Ar-H), 6.66 (1H, s, Ar-H). UV data, λ_{max}, nm: 382.

Indole-3-carboxaldehyde-2-hydroxy benzhydrazone (2)

Pale yellow. MF, $C_{16}H_{13}N_3O_2$. mp, 250-252°C. MS, m/z: 280 [M]+. IR, ν, cm^{-1}: 3373 (O-H), 3125 (N-H), 1625 (C=O), 1602 (C=N). 1H NMR, δ, ppm: 12.31 (1H, s, -NH), 11.65 (1H, s, OH), 8.65 (1H, s, HC=N), 8.32-8.30 (1H, d, Ar-H), 7.96- 7.94 (1H, d, Ar-H), 7.88- 7.87 (1H, d, Ar-H), 7.47- 7.42 (2H, m, Ar-H), 7.24- 7.15 (2H, m, Ar-H), 6.98 – 6.94 (2H, t, Ar-H). UV data, λ_{max}, nm: 337.

o-Vanillin-4-bromobenzhydrazone (3)

Pale yellow. MF, $C_{15}H_{13}N_2O_3Br$. mp, 152-154°C. MS, m/z: 349 [M]+, 351 [M+2]+. IR, ν, cm^{-1}: 3560 (O-H), 3212 (N-H), 1650 (C=O), 1605 (C=N). 1H NMR, δ, ppm: 12.13 (1H, s, -NH), 10.86 (1H, s, -OH), 8.65 (1H, s, HC=N), 7.90-7.88 (2H, d, Ar-H), 7.78-7.76 (2H, d, Ar-H), 7.14- 7.12 (1H, d, Ar-H), 7.05- 7.03 (1H, d, Ar-H), 6.93 – 6.85 (1H, m, Ar-H), 3.82 (3H, s, $-OCH_3$). UV data, λ_{max}, nm: 358.

o-Vanillin-4-chlorobenzhydrazone (4)

Colourless. MF, $C_{15}H_{13}N_2O_3Cl$. mp, 162-164°C. MS, m/z: 304 [M]+. IR, ν, cm^{-1}: 3553 (O-H), 3209 (N-H), 1648 (C=O), 1604 (C=N). 1H NMR, δ, ppm: 12.14 (1H, s, -NH), 10.88 (1H, s, -OH), 8.66 (1H, s, HC=N), 7.98-7.95 (2H, d, Ar-H), 7.64- 7.62 (2H, d, Ar-H), 7.18- 7.16 (1H, d, Ar-H), 7.05- 7.03 (1H, d, Ar-H), 6.89 – 6.85 (1H, t, Ar-H), 3.82 (3H, s, $-OCH_3$). UV data, λ_{max}, nm: 358.

o-Vanillin-2-hydroxybenzhydrazone (5)

Pale yellow. MF, $C_{15}H_{14}N_2O_4$. mp, 188 °C. MS, m/z: 287 [M]+. IR, ν, cm^{-1}: 3408 (O-H), 3226 (N-H), 1650 (C=O), 1603 (C=N). 1H NMR, δ, ppm: 12.02 (1H, s, -OH), 11.78 (1H, s, -OH), 10.87 (1H, s, N-H), 8.71 (1H, s, HC=N), 7.91-7.89 (1H, d, Ar-H), 7.44-7.43 (1H, t, Ar-H), 7.16 (1H, d, Ar-H), 7.06- 7.04 (1H, d, Ar-H), 7.00 – 6.97 (2H, t, Ar-H), 6.89-6.86 (1H, t, Ar-H), 3.82 (3H, s, $-OCH_3$). UV data, λ_{max}, nm: 370.

o-Vanillin-3-nitrobenzhydrazone (6)

Pale yellow. MF, $C_{15}H_{13}N_3O_5$. mp, 178-180°C. MS, m/z: 316 [M]+, 317 [M+1]+. IR, ν, cm^{-1}: 3249 (O-H), 3082 (N-H),1648 (C=O), 1603 (C=N). 1H NMR, δ, ppm: 12.36 (1H, s, -NH), 10.72 (1H, s, -OH), 8.99 (1H, s, HC=N), 8.79 (1H, s, Ar-H), 8.47-8.45 (1H, d, Ar-H), 8.40-8.38 (1H, d, Ar-H), 7.88- 7.86 (1H, d, Ar-H), 7.22- 7.20 (1H, d, Ar-H), 7.07 – 7.05 (1H, d, Ar-H), 6.90- 6.86 (1H, t, Ar-H), 3.82 (3H, s, $-OCH_3$). UV data, λ_{max}, nm: 358.

o-Vanillin-4-nitrobenzhydrazone (7)

Yellow. MF, $C_{15}H_{13}N_3O_5$. mp, 186-188°C. MS, m/z: 316 [M]+, 317 [M+1]+. IR, ν, cm^{-1}: 3531 (O-H), 3207 (N-H), 1651 (C=O), 1597 (C=N). 1H NMR, δ, ppm: 12.33 (1H, s, -NH), 10.72 (1H, s, -OH), 8.70 (1H, s, HC=N), 8.40-8.38 (2H, d, Ar-H), 8.19-8.17 (2H, d, Ar-H), 7.22- 7.20 (1H, d, Ar-H), 7.06- 7.05 (1H, d, Ar-H), 6.90 – 6.86 (1H, t, Ar-H), 3.83 (3H, s, $-OCH_3$). UV data, λ_{max}, nm: 339.

Pyridoxal-4-bromobenzhydrazone (8)

Pale yellow. MF, $C_{15}H_{14}N_3O_3Cl$. mp, 240-242°C. MS, m/z: 364 [M]+, 366 [M+2]+. IR spectrum, ν, cm^{-1}: 1694 (C=O), 1584 (C=N). 1H NMR, δ, ppm: 13.33 (1H, s, -NH), 9.10 (1H, s, HC=N), 8.22 (1H, s, Ar-H), 8.02-8.00 (2H, d, Ar-H), 7.82- 7.80 (2H, d, Ar-H), 4.78 (2H, s, Ar-CH_2), 2.64 (3H, s, $-CH_3$). UV data, λ_{max}, nm: 351.

Pyridoxal-4-chlorobenzo hydrazone (9)

Pale yellow. MF, $C_{15}H_{14}N_3O_3Br$. mp, 220-222°C. MS, m/z: 319 [M]+. IR, ν, cm^{-1}: 3247 (O-H), 3088 (N-H), 1682 (C=O), 1623 (C=N). 1H NMR, δ, ppm: 13.27 (1H, s, -N]H), 9.08 (1H, s, HC=N), 8.22 (1H, s, Ar-H), 8.09-8.07 (2H, d, Ar-H), 7.69- 7.66 (2H, d, Ar-H), 4.77 (2H, s, Ar-CH_2), 2.63 (3H, s, -CH_3). UV data, λ_{max}, nm: 351.

Pyridoxal-3-nitrobenzhydrazone (10)

Pale yellow. MF, $C_{15}H_{14}N_4O_5$. mp, 198-200°C. MS: m/z: 331 [M]+. IR, ν, cm^{-1}: 3317 (O-H), 3084 (N-H), 1682 (C=O), 1612 (C=N). 1H NMR, δ, ppm: 13.51 (1H, s, -NH), 9.11 (1H, s, HC=N), 8.86 (1H, s, Ar-H), 8.52-8.50 (2H, d, Ar-H), 8.24 (1H, s, Ar-H), 7.91-7.87 (1H, t, Ar-H), 4.80 (2H, s, -CH_2 -), 2.64 (3H, s, -CH_3). UV data, λ_{max}, nm: 349.

Pyridoxal-4-nitrobenzhydrazone (11)

Pale yellow. MF, $C_{15}H_{14}N_4O_5$. mp, 248-250°C. MS, m/z: 331 [M]+. IR, ν, cm^{-1}: 1693 (C=O), 1604 (C=N). 1H NMR, δ, ppm: 13.42 (1H, s, NH), 12.96 (1H, s, -OH), 9.09 (1H, s, HC=N), 8.43-8.41(2H, d, Ar-H), 8.29-8.27 (2H, d, Ar-H), 8.23 (1H, s, Ar-H), 4.78(2H, s, -CH_2 -), 2.62 (3H, s, -CH_3). UV data, λ_{max}, nm: 351.

2.4. Biological activity studies:

2.4.1. Antibacterial activity:

By employing the well diffusion method, the antibacterial activity of the Schiff base was investigated against the following bacteria: *Bacillus licheniformis* (CP000002.3), *Staphylococcus epidermidis* (MTCC 435), *Pseudomonas syringae* (MTCC 1604), and *Klebsiella pneumoniae* (MTCC 39). The stock sample solutions were made in DMSO (1 mg/mL). 100 µL of 24 hour bacterial culture was inoculated onto Mueller Hinton Agar medium taken in petri plates. The plates were set aside for ten minutes to allow for adsorption. Wells were created using a sterile plastic borer with a diameter of 8 mm and 100 µL of the sample solutions were placed inside of them. After 24 hours of incubation at 37°C, the zones of inhibition on the plates were measured in millimetres. The standard drug used was Ampicillin (100 µg/mL) and the negative control was DMSO.

2.4.2. Antioxidant activity:

The *in vitro* antioxidant activity of the compounds **1-11** was evaluated by the DPPH (1,1-diphenyl-2-picrylhydrazyl) method. Stock solutions of the compounds were prepared in DMSO (1 mg/mL) from which 20, 40, 60, 80 and 100 µL were diluted to 1 mL using absolute alcohol. 4 mL of DPPH solution (0.4 mM) was added to each of these solutions, so as to get the final volume to 5 mL. DPPH alone in ethanol was used as a positive control and Ascorbic acid was used as a reference radical scavenger. The solutions were vortexed and incubated in dark at room temperature for 30 minutes. A decrease in absorbance of DPPH in all the sample solutions was measured at 517 nm

using UV-Visible spectrophotometer[10]. The DPPH free radical scavenging activity was calculated in terms of DPPH scavenging effect (%) using the formula

$$\text{DPPH scavenging effect (\%)} = \frac{Ao - Ac}{Ao} \times 100$$

where A_o and A_c are the absorbance values of the control and the sample respectively. IC_{50} (the concentration required to cause 50% of DPPH scavenging effect) values for each sample were calculated from their respective DPPH scavenging effects at various concentrations.

2.4.3. Anti-inflammatory activity:

The *in vitro* anti-inflammatory activity of the Schiff bases was studied using inhibition of Bovine Serum Albumin (BSA) denaturation assay. Varying volumes of the test samples (50, 100, 200, 300 and 500 µL) were added from their stock solution (1 mg/mL) to 0.2 mL of 1 % BSA and the final volume of each reaction mixture was made to 5 mL using sodium phosphate buffer (pH 6.3). The reaction mixtures were properly mixed and incubated at 37°C for 20 min. Later they were heated at 70°C for 5 min. After cooling, the turbidity of each sample was measured at 660 nm using a UV-Visible spectrophotometer. Diclofenac sodium was used as a standard drug and a solution of phosphate buffer was used as a control[11,12]. The percentage inhibition of protein denaturation was calculated by using the formula,

$$\text{Percentage inhibition} = [(A_{Control} - A_{Sample})/A_{Control}] \times 100.$$

IC_{50} (the concentration required to cause 50% inhibition of BSA denaturation) values (µM) for each sample were calculated.

2.5. Docking studies:

2.5.1. Ligand Preparation: Compound structures were drawn in the Maestro build panel and then prepared with the LigPrep module. Various conformers were generated using the OPLS-4 force field and docking studies were conducted using the low energy conformers of each ligand.

2.5.2. Protein Preparation: Penicillin-binding protein 3 (PBP3), in its three-dimensional crystal structure (pdb id: 8GPW, resolution 2.06Å), was obtained from *Klebsiella pneumoniae*. Hydrogen atoms were added and unnecessary water molecules were eliminated during the protein preparation process, which was carried out using the protein preparation wizard module and default settings.

2.5.3. Docking: The docking investigations were conducted using the grid-based ligand docking technique, GLIDE, from the Schrödinger programme[13]. Using a receptor grid creation panel found in the GLIDE, a grid was first made inside a cubic box, centred on the co-crystallized ligand. In the case of non-polar atoms with a partial charge cut-off of

0.25, the default VanderWaals scaling was set to 0.9[14]. Subsequently, the molecules underwent extra precision (XP) protocol docking.

3. Results and discussion:

3.1. Chemistry:

The Schiff base compounds were prepared by the condensation of aromatic aldehydes with substituted benzhydrazides. The completion of the reaction and the purity of the Schiff bases was tested by TLC technique. They are coloured, stable to air and atmospheric moisture. The Schiff bases are soluble in organic solvents like DMSO, but insoluble in water. The Schiff bases were characterised by ESI-MS, UV-Vis, FTIR and ^{1}H NMR spectroscopic techniques.

Table 1. Comparison of yields under different reaction conditions

Schiff base	**Conventional reflux**		**Reflux in ionic liquid**	
	Time (h)	% Yield	Time (min)	% Yield
Furfural-2-hydroxybenzhydrazone (**1**)	3	50	40	72
Indole-3-carboxaldehyde-2-hydroxybenz-hydrazone (**2**)	3	62	35	78
o-Vanillin-4-bromobenzhydrazone (**3**)	2	57	25	74
o-Vanillin-4-chlorobenzhydrazone (**4**)	2	57	25	76
o-Vanillin-2-hydroxybenzhydrazone (**5**)	2	71	20	83
o-Vanillin-3-nitrobenzhydrazone (**6**)	2	58	35	71
o-Vanillin-4-nitrobenzhydrazone (**7**)	2	53	40	70
Pyridoxal-4-bromobenzhydrazone (**8**)	2	58	25	77
Pyridoxal-4-chlorobenzhydrazone (**9**)	2	50	30	72
Pyridoxal-3-nitrobenzhydrazone (**10**)	2	52	25	71
Pyridoxal-4-nitrobenzhydrazone (**11**)	2	46	30	75

3.1.1. ESI-MS:

Mass spectra of the Schiff bases were recorded to determine their molecular weights. Mass spectra showed prominent peaks corresponding to the calculated molecular weights of the compounds and are consistent with the proposed molecular formulas.

3.1.2. IR:

The FTIR spectra showed the stretching vibration frequencies as expected. All the Schiff bases displayed a band around 1600 cm^{-1} for azomethine (HC=N) stretching vibration. The compounds exhibited bands in the range of 3200-3550 cm^{-1}, 3000-3250 cm^{-1}, 1625-1700 cm^{-1} and 1100-1250 cm^{-1} for the stretching frequencies of O-H, N-H, C=O and C-O respectively. The mass and FTIR data are depicted in table 2.

Table 2. ESI-Mass and FTIR (cm^{-1}) spectral data

Compound	Mol. Wt. Calc. (Obs.)	ν(O-H)	ν (N-H)	ν (C=O)	ν (C=N)	ν (C-O)
1	230.23 (231.6)	3394	3141	1631	1604	1131
2	280.72 (280.8)	3373	3125	1625	1602	1103
3	349.18 (349.3)	3560	3212	1650	1605	1239
4	304.73 (305.3)	3553	3209	1648	1604	1238
5	286.3 (287.8)	3408	3226	1650	1603	1152
6	315.28 (316.4)	3249	3082	1648	1603	1244
7	315.28 (316.3)	3531	3207	1651	1597	1242
8	364.19 (364.8)	3237	3026	1694	1584	1157
9	319.74 (320.8)	3247	3088	1682	1623	1159
10	330.29 (331.8)	3317	3084	1682	1612	1152
11	330.29 (331.8)	3259	3046	1693	1604	1161

3.1.3. ^{1}H NMR:

Proton nuclear magnetic resonance spectra of all the Schiff bases were recorded in DMSO-d_6. The ^{1}H NMR spectra showed a signal between 8.37 and 9.11 ppm for azomethine (HC=N) protons which confirms the successful formation of Schiff bases. The phenolic protons in compounds **1-7** have appeared at 11.65 to 12.36 ppm as singlets, while for the compounds **8-11** at 13.27 to 13.51 ppm. The -NH protons for the **1-7** and **14** are observed between 10.72 to 12.96, while for the compounds **8-10** their signal has disappeared maybe due to their exchange with deuterium[15]. Except for the compounds **1, 2** and **5**, the signals for aromatic ring protons for other compounds are seen from 6.85 to 8.80 ppm. The higher peak values for Ar-H is attributed to the presence of electron withdrawing groups on the benzene ring of benzhydrazides which lead to their deshielding. The singlets at 3.82 ppm indicate -OCH_3 protons of o-Vanillin in **3-7**. Singlets at 4.78 and 2.63 ppm suggest Ar-CH_2 and -CH_3 protons in pyridoxal for the compounds **8-11**. The signal for the alcoholic proton between 4-5 ppm in pyridoxal (**8-11**) has disappeared which is expected with deuterium exchange.

3.1.4. UV-Vis:

The UV-Visible spectra of the compounds **1-11** were recorded in DMSO. All the compounds exhibited λ_{max} value between 300-400 nm corresponding to the $\pi \rightarrow \pi^*$ transition of the aromatic chromophore and $n \rightarrow \pi^*$ transition of the azomethine HC=N group. The electronic spectra of the compounds are presented in figure 1. ESI-Mass, 1H NMR, FT-IR and UV-Vis spectra of all the compounds **1-11** are presented in figures S1-S44.

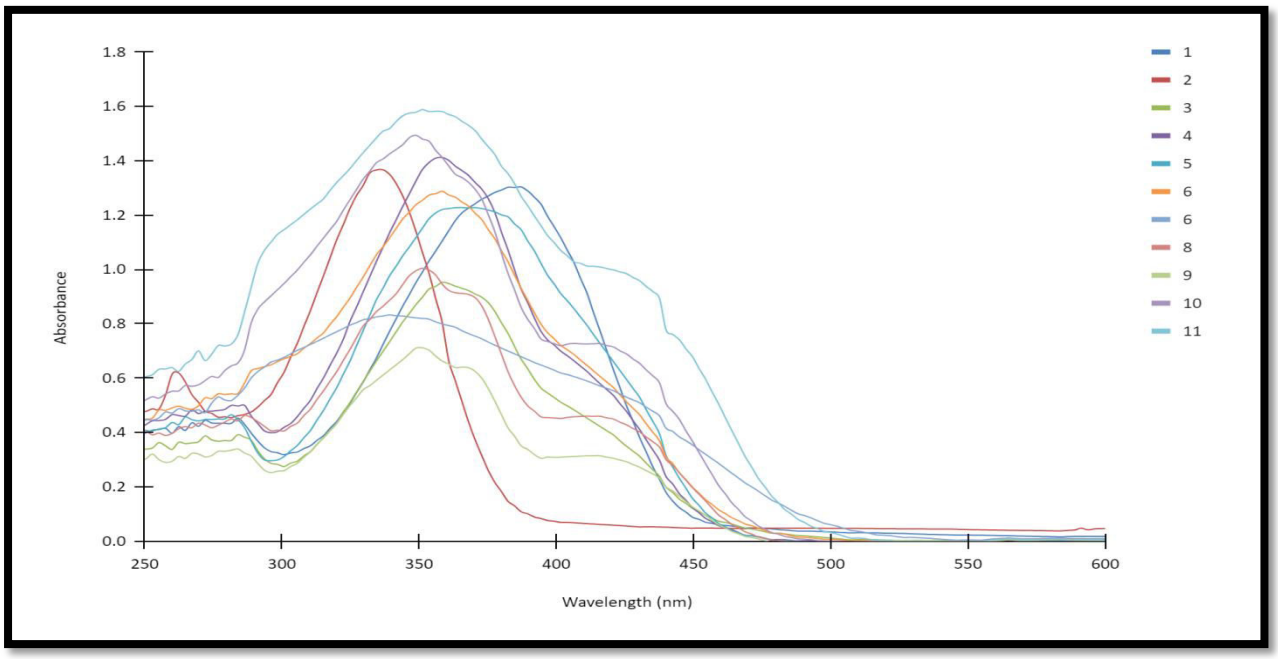

Fig.1. UV-Visible spectra of Schiff bases

Based on the spectral data the structures of the compounds are given in figure 2.

Fig. 2. Structures of Schiff bases

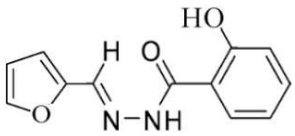

1

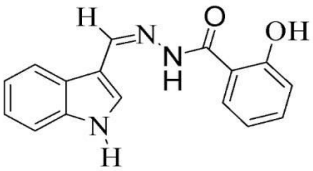

2

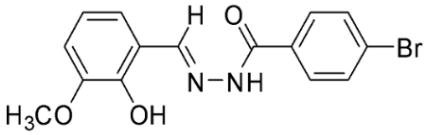

3

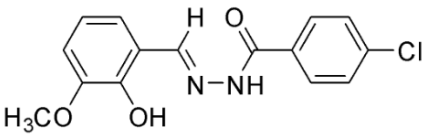

4

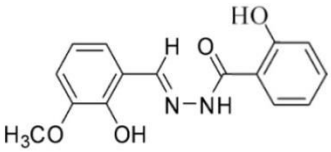

5

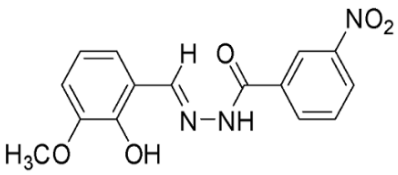

6

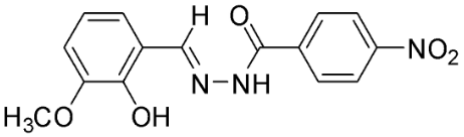

7

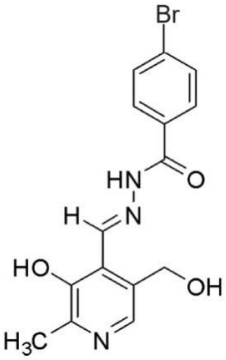

8

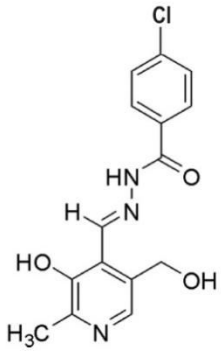

9

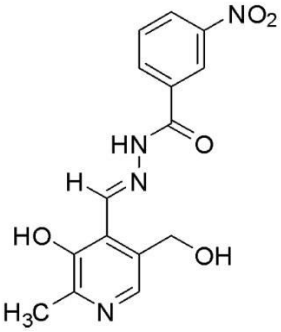

10

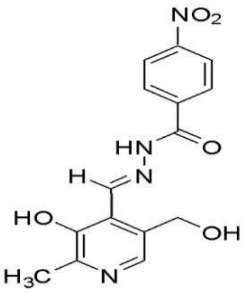

11

3.2. Biological activity:

3.2.1. Antibacterial activity:

All of the compounds in this study were tested for their antibacterial potential against Gram-positive (*B. licheniformis and S. epidermidis*) and Gram-negative (*P. syringae and K. pneumoniae*) bacteria by the well diffusion method. The antibiotic ampicillin (100 µg/ml) was used as a positive control. The outcome of antibacterial evaluation indicates that all of them are able to inhibit the growth of Gram positive bacteria with varied activity. *P. syringae* is resistant to most of them except **1**, **3** and **4**. But all the compounds are able to inhibit the growth of *K. pneumoniae*. The inhibition zone values of the Schiff bases are summarised in Table 3.

Table 3: Zone of inhibition (mm) of Schiff bases

Bacteria	**Zone of inhibition (mm)**											
	1	**2**	**3**	**4**	**5**	**6**	**7**	**8**	**9**	**10**	**11**	**Ampicillin**
B. licheniformis CP000002.3	12	11	18	10	20	16	15	10	09	08	15	25
S. epidermidis MTCC 435	13	12	20	09	19	11	17	08	12	07	10	23
P. syringae MTCC 1604	08	-	08	18	-	-	-	-	-	-	-	21
K. pneumoniae MTCC 39	15	10	14	12	12	10	07	13	16	13	14	24

3.2.2. Antioxidant activity:

DPPH is a stable free radical and the scavenging activity of the samples is assayed by measuring a decrease in absorbance of DPPH at 517 nm. The DPPH method is based on the electron donation by an antioxidant to neutralise the DPPH free radical[16]. The reaction is indicated by a change in the purple colour of DPPH, which was observed with all the samples. The absorbance data obtained was used to calculate the DPPH scavenging effect (%) from which the IC_{50} values are calculated and presented in table 4. These values demonstrate the effective free radical scavenging ability of the sample compounds and thereby reduce the effects of oxidative stress in biological systems.

Table 4: IC_{50} values for the antioxidant activity

Sample	1	2	3	4	5	6	7	8	9	10	11	Ascorbic acid
IC_{50} (µM)	21.02	48.44	37.80	19.03	12.57	43.77	60.32	32.51	36.27	36.93	47.83	2.04

3.2.3. Anti-inflammatory activity:

All the synthesised Schiff base compounds were investigated for the anti-inflammatory activity by the inhibition of heat induced denaturation of bovine serum albumin (BSA). The drug Diclofenac sodium was used as a standard. All the compounds exhibited a concentration dependent protein denaturation inhibition. From the absorbance data collected at 660 nm, percentage inhibition of BSA denaturation for the various concentrations was calculated, from which IC_{50} values were obtained. Table 5 depicts the IC_{50} values (µM), which shows that all the compounds possess less activity compared to Diclofenac and the compound **5** exhibits lowest inhibitory concentration.

Table 5: IC_{50} values for the anti-inflammatory activity

Sample	1	2	3	4	5	6	7	8	9	10	11	Diclofenac
IC_{50} (µM)	121.61	102.59	94.5	85.32	67.41	122.11	71.68	77.43	81.31	92.64	84.77	27.53

3.3. Docking:

To understand the molecular interactions between inhibitors with Penicillin-binding protein 3 (PBP3) of Klebsiella pneumoniae, crystal structure of PBP3 (pdb id: 8GPW) was downloaded from the protein data bank. GLIDE 9.1 was used for molecular docking[17]. All the molecules in the present study docked at the centre of the penicillin binding site and showed hydrogen bond interactions with amino acid residues THR 497, SER 307, GLY 543. Docking results of molecules showed appreciable scores and better than the standard Ampicillin. The dock scores of the molecules are provided in table 6, the highest dock score was shown by molecule o-Vanillin-2-hydroxybenzhydrazone or **5** (-8.686 kcal/mol). The high binding affinity of molecule **5** can be attributed to additional π -π stacking interaction with amino acid residue TYR 541 and the molecule's high dock score shows these additional π -π stacking along with hydrogen bond interactions. Dock pose and ligand interaction of molecule **5** is shown in figure 2.

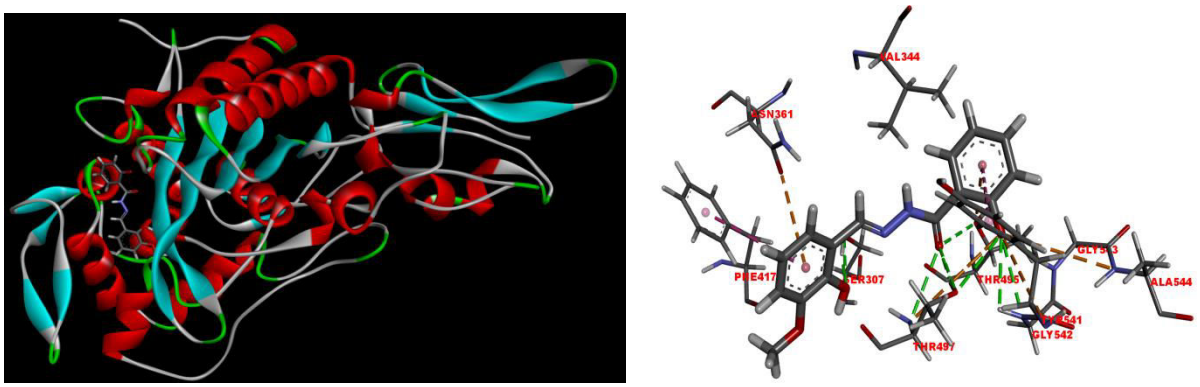

(a) *(b)*

Fig. 3. (a) o-Vanillin-2-hydroxybenzhydrazone (tube form) with receptor Penicillin-binding protein 3 (PBP3) of *Klebsiella pneumoniae* (ribbon form) (b) Hydrogen bond interaction and Hydrophobic interactions between o-Vanillin-2-hydroxybenzhydrazone and receptor Penicillin-binding protein 3 (PBP3) of Klebsiella pneumoniae

Table 6: Dock scores of molecules

Molecule	5	8	9	2	1	11	10	6	7	3	4	Ampicillin
XP Dock Score (kcal/mol)	-8.686	-7.848	-7.432	-7.265	-6.560	-6.262	-5.613	-5.356	-5.226	-5.012	-5.119	-4.347

Conclusion

Eleven Schiff bases with substituted benzhydrazides have been successfully synthesised by a greener method in the presence of an ionic liquid. The structures of the compounds were confirmed by ESI-Mass, NMR, FT-IR and UV-Vis spectroscopy. The antibacterial activity assay suggests that the compounds have moderate to good inhibition activity against gram positive bacteria *B. licheniformis, S. epidermidis* and also one gram negative bacteria *K. pneumoniae*. They also displayed free radical scavenging and anti-inflammatory activities.

Acknowledgements

The authors extend their gratitude to the Management, St Francis College for Women, Hyderabad, for providing the financial support to perform this research work.

References

1. Adebimpe, D.A (2023). Synthesis of Schiff Bases by Non-Conventional Methods. Schiff Base in Organic, Inorganic and Physical Chemistry, 436.
2. Lemilemu, F., Bitew, M., Demissie, T.B (2021). Synthesis, antibacterial and antioxidant activities of Thiazole-based Schiff base derivatives: a combined experimental and computational study. BMC Chemistry, 15, 67.
3. Ahmed, I.A.S., Mostafa, S., Mahmoud, M.E., Osama, Y., Mostafa, A., Adel, M. K., Aboel-Magd, A.A., Josef, W., Markus, B., Pedram, F., Mahmoud, S.T (2022). Base-Free Synthesis and Photophysical Properties of New Schiff Bases Containing Indole Moiety. ACS Omega, *7* (12), 10178-10186.
4. Koteswara Rao, V., Subba Reddy, S., Satheesh Krishna, B., Reddi Mohan Naidu, K., Naga Raju, C., Ghosh, S.K (2010). Synthesis of Schiff's bases in aqueous medium: a green alternative approach with effective mass yield and high reaction rates, Green Chemistry Letters and Reviews, 3:3, 217-223.
5. Deepjyoti, D., Nayan Kamal, B., Joydeep, B (2021). A review on synthesis and biological activity of Schiff Bases. Indian Journal of Chemistry, 60B, 1478-1489.
6. Satish, B.M., Rakesh, K.M., Kalpesh, S.M., Prajal, P.M., Siddhesh, S.D (2023). Microwave-Assisted Rapid and Green Synthesis of Schiff Bases Using Cashew Shell Extract as a Natural Acid Catalyst. ACS Omega, *8* (1), 473-479.
7. Kharissova, O.V., Kharisov, B.I., Oliva González, C.M., Méndez, Y.P., López, I (2019). Greener synthesis of chemical compounds and materials. Royal Society open science, 6: 191378.
8. Sinha, B., Saha, S (2020). Imidazolium Ionic Liquid-Supported Schiff Base and Its Transition Metal Complexes: Synthesis, Physicochemical Characterization and Exploration of Antimicrobial Activities. Solvents, Ionic Liquids and Solvent Effects. 863.
9. Susmitha, K., Sumalatha, D (2023). Green synthesis, DFT and molecular docking studies of 4-amino indane derived Schiff bases. Materials today: Proceedings. (Article in press)
10. Afzal, H.R., Khan, N.U.H., Sultana, K., Mobashar, A., Lareb, A., Khan, A., Gull, A., Afzaal, H., Khan, M.T., Rizwan, M., Imran, M (2021). Schiff Bases of Pioglitazone Provide Better Antidiabetic and Potent Antioxidant Effect in a Streptozotocin-Nicotinamide-Induced Diabetic Rodent Model. ACS Omega, 3;6(6): 4470-4479.
11. Chirumamilla, P., Taduri, S (2023). Assessment of in vitro anti-inflammatory, antioxidant and antidiabetic activities of *Solanum khasianum* Clarke. Vegetos, 36, 575–582.
12. Gunathilake, K.D.P.P., Ranaweera, K.K.D.S., Rupasinghe, H.P.V (2018). In Vitro Anti-Inflammatory Properties of Selected Green Leafy Vegetables. Biomedicines, *6*, 107.
13. Schrödinger LLC Glide, Version 9.1. New York, NY. (Evaluation version)

14. Halgren, T.A., Murphy, R.B., Friesner, R.A., Beard, H.S., Frye, L.L., Pollard, W.T., Banks, J.L (2004) Glide: a new approach for rapid, accurate docking and scoring. 2. Enrichment factors in database screening. J Med Chem 47(7):1750–1759.
15. Nikola, Z.K., Vukadin, M.L., Violeta, S.J., Grgurić-Sipka, S., Sabo, T (2003). Platinum(IV) complex with pyridoxal semicarbazone. Inorganic Chemistry Communications, 6. 561-564.
16. Bedlovičová, Z., Strapáč, I., Baláž, M., Salayová, A (2020). A Brief Overview on Antioxidant Activity Determination of Silver Nanoparticles. Molecules, *25*, 3191.
17. Friesner, R,A., Banks, J.L., Murphy, R.B., Halgren, T.A., Klicic, J.J., Mainz, D.T., Repasky, M.P., Knoll, E.H., Shelley, M., Perry, J.K., Shaw, D.E., Francis, P, Shenkin, P.S (2004). Glide: a new approach for rapid, accurate docking and scoring. 1. Method and assessment of docking accuracy. J Med Chem, 47(7):1739-49

Supplementary material

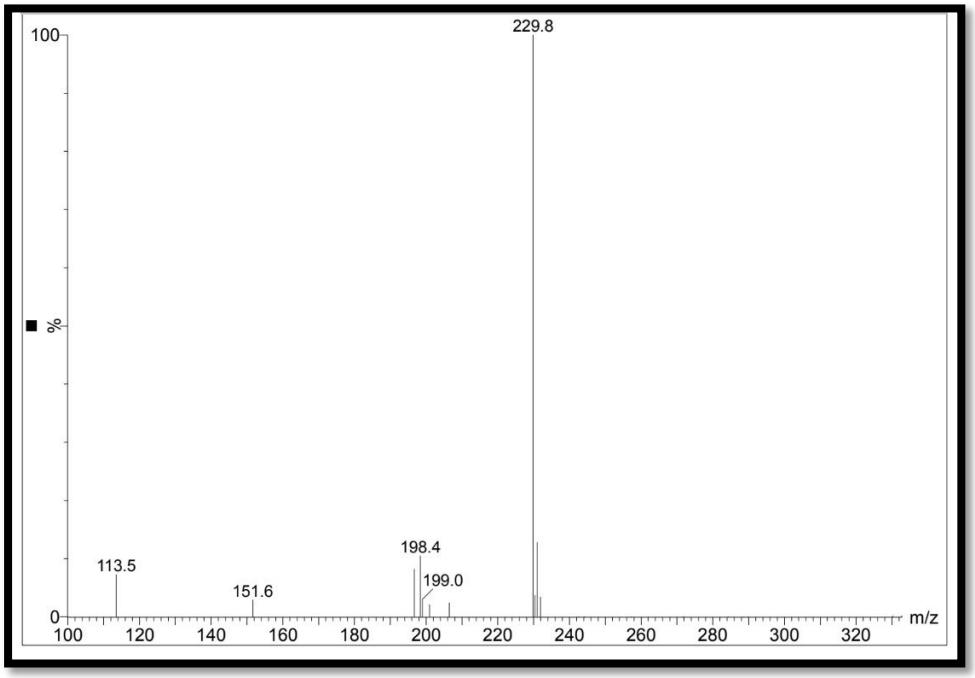

Fig. S1. Mass spectrum of Furfural-2-hydroxy benzhydrazone

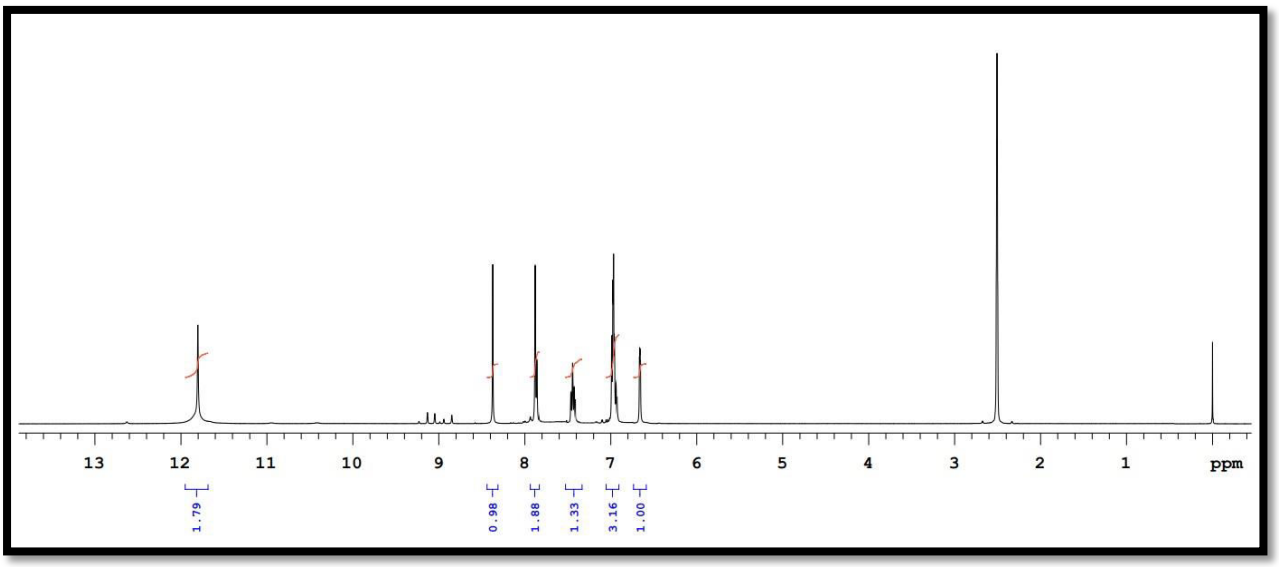

Fig. S2. 1H NMR spectrum of Furfural-2-hydroxy benzhydrazone

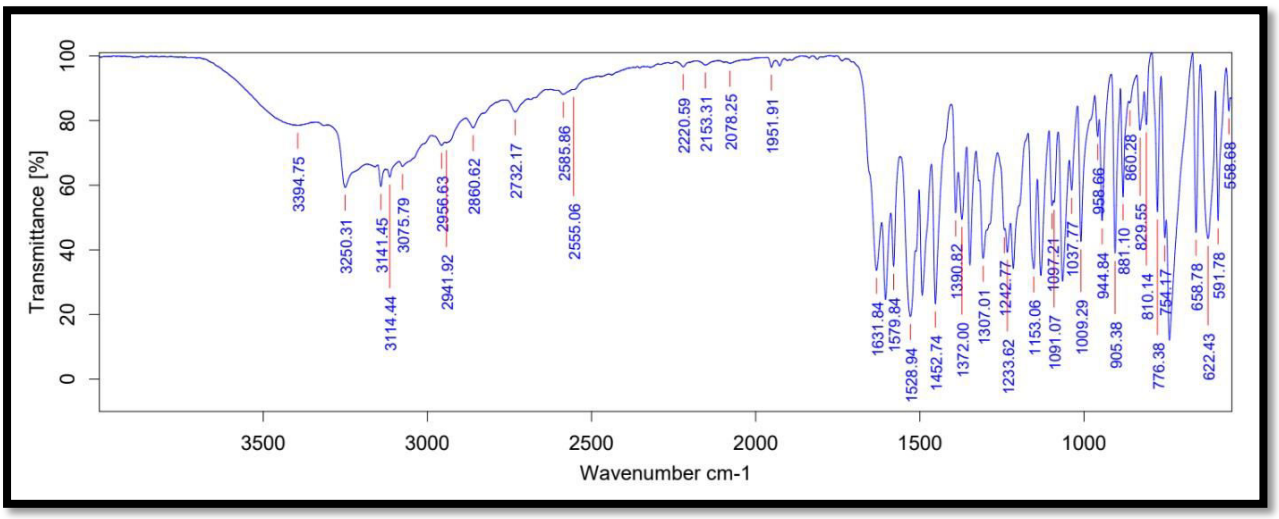

Fig. S3. IR spectrum of Furfural-2-hydroxy benzhydrazone

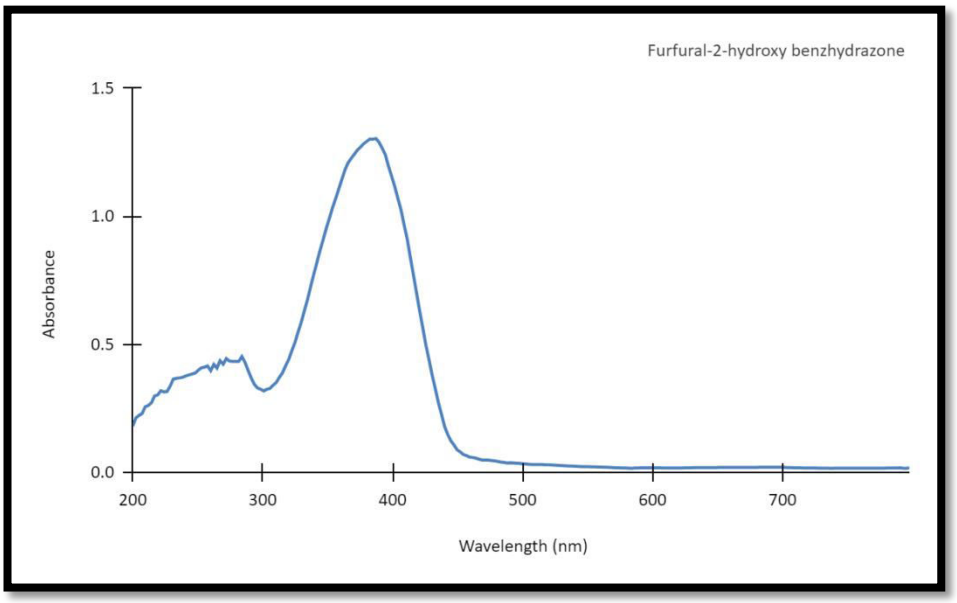

Fig. S4. UV-Vis spectrum of Furfural-2-hydroxy benzhydrazone

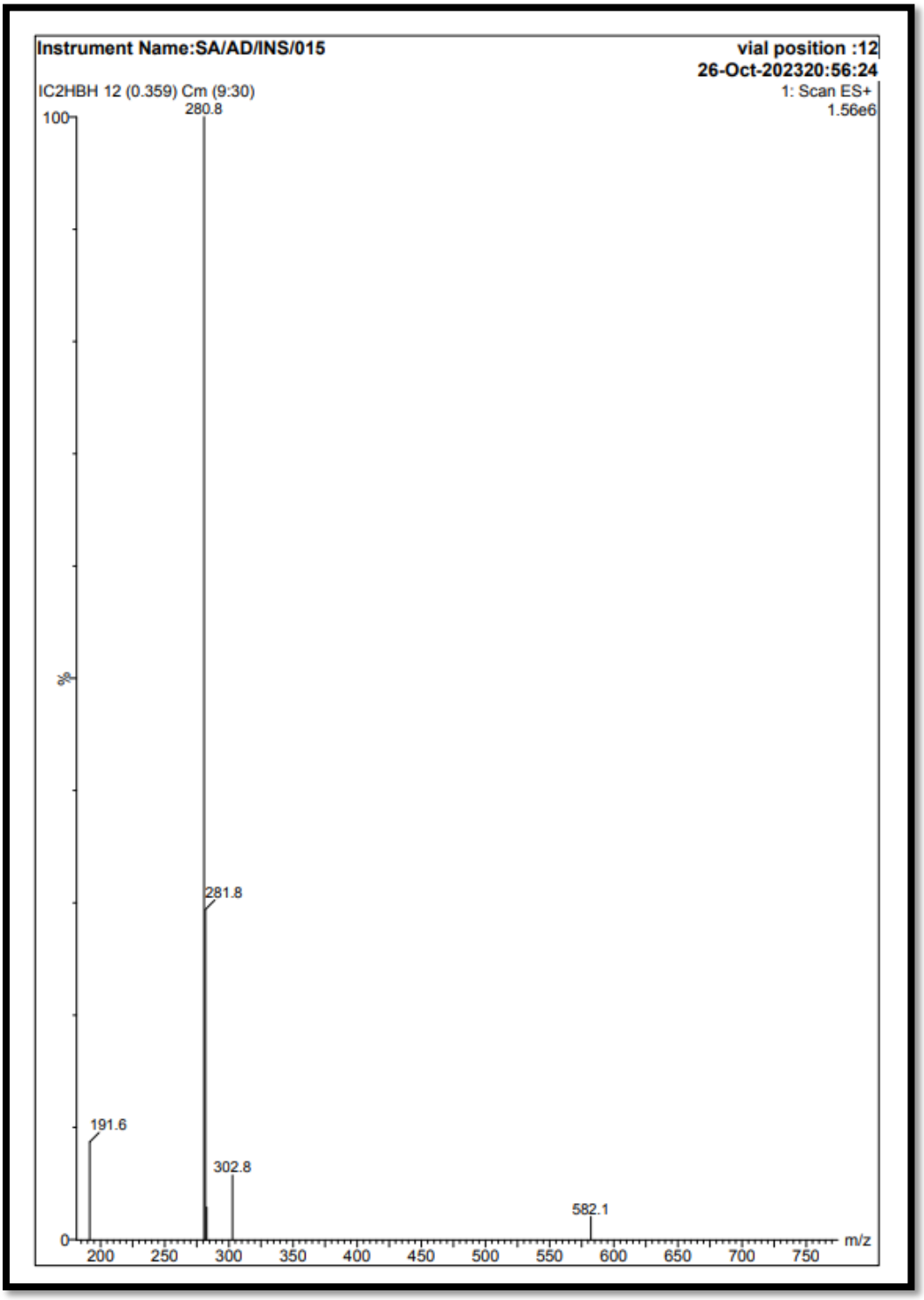

Fig. S5. Mass spectrum of Indole-3-carboxaldehyde-2-hydroxy benzhydrazone

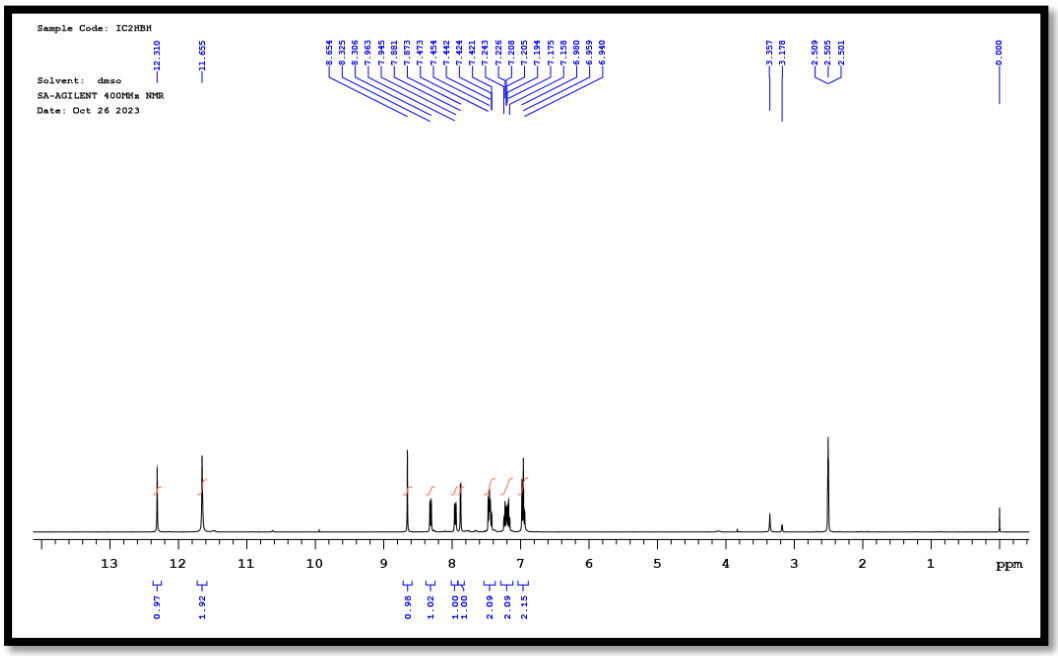

Fig. S6. 1H NMR spectrum of Indole-3-carboxaldehyde-2-hydroxy benzhydrazone

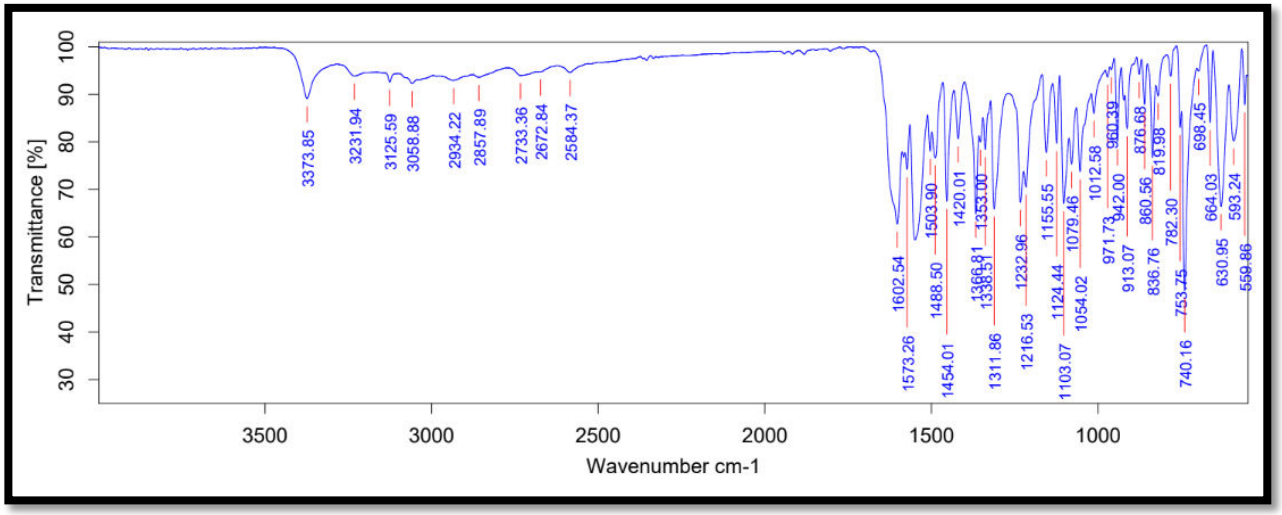

Fig. S7. IR spectrum of Indole-3-carboxaldehyde-2-hydroxy benzhydrazone

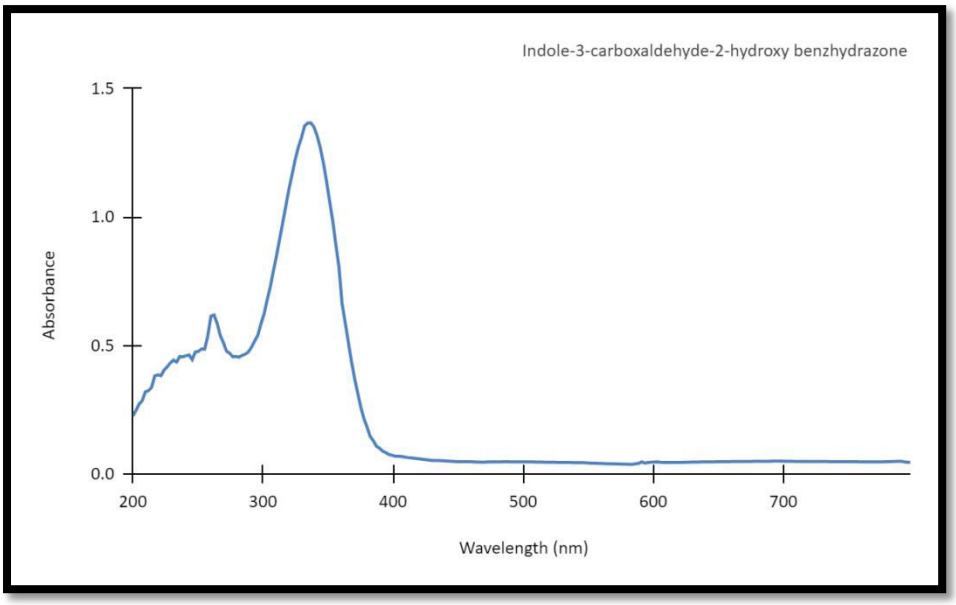

Fig. S8. UV-Vis spectrum of Indole-3-carboxaldehyde-2-hydroxy benzhydrazone

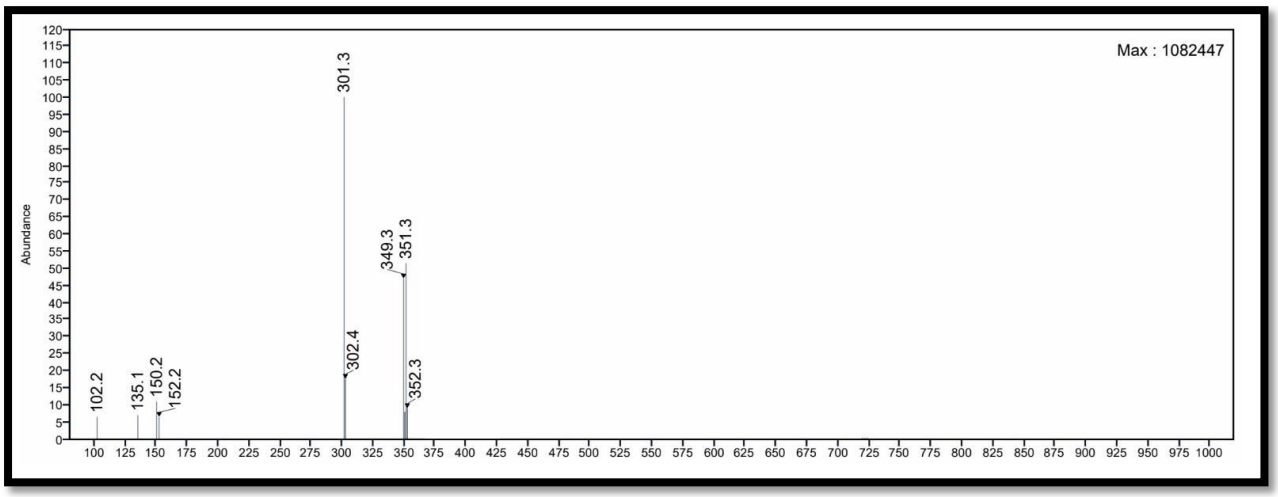

Fig. S9. Mass spectrum of o-Vanillin-4-bromo benzhydrazone

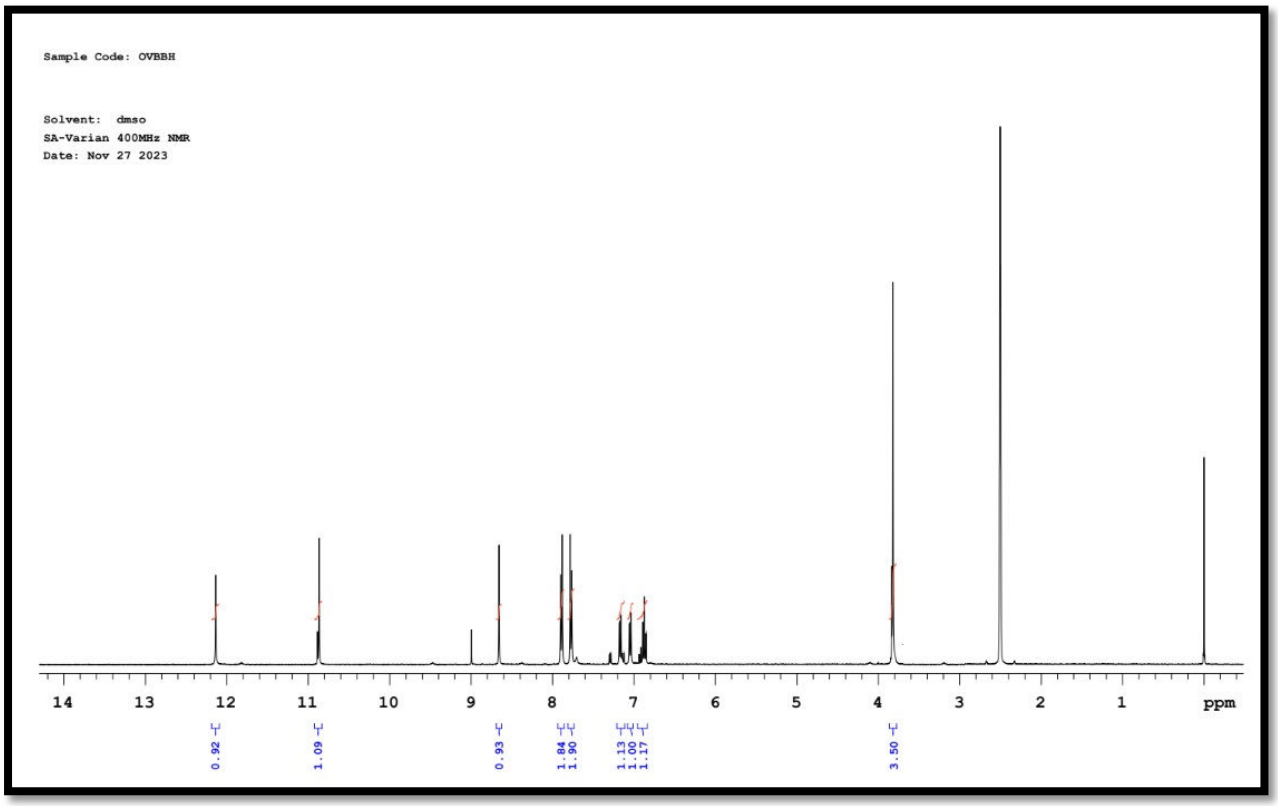

Fig. S10. 1H NMR spectrum of o-Vanillin-4-bromo benzhydrazone

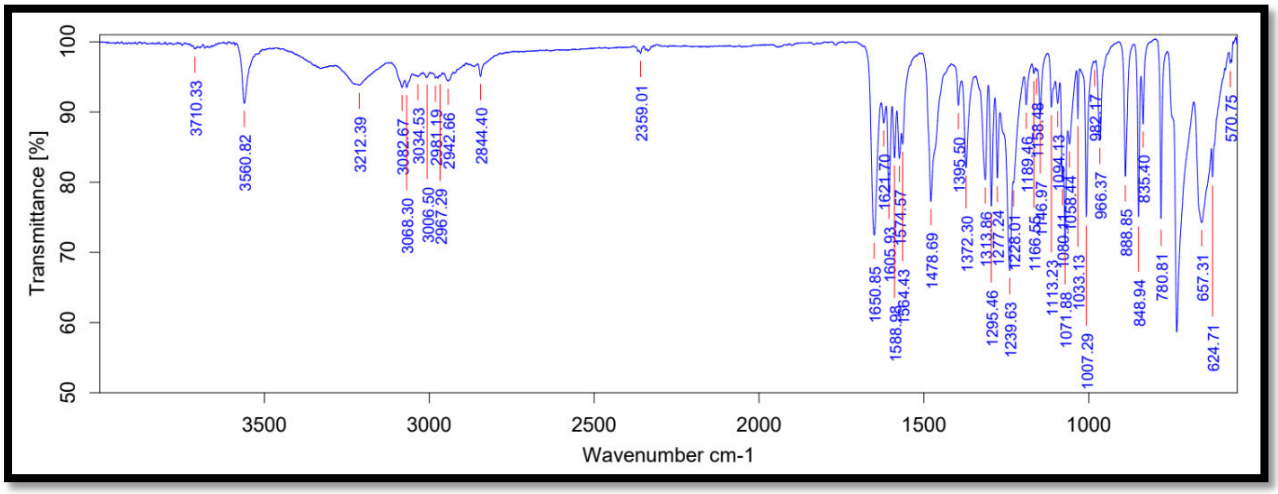

Fig. S11. IR spectrum of o-Vanillin-4-bromo benzhydrazone

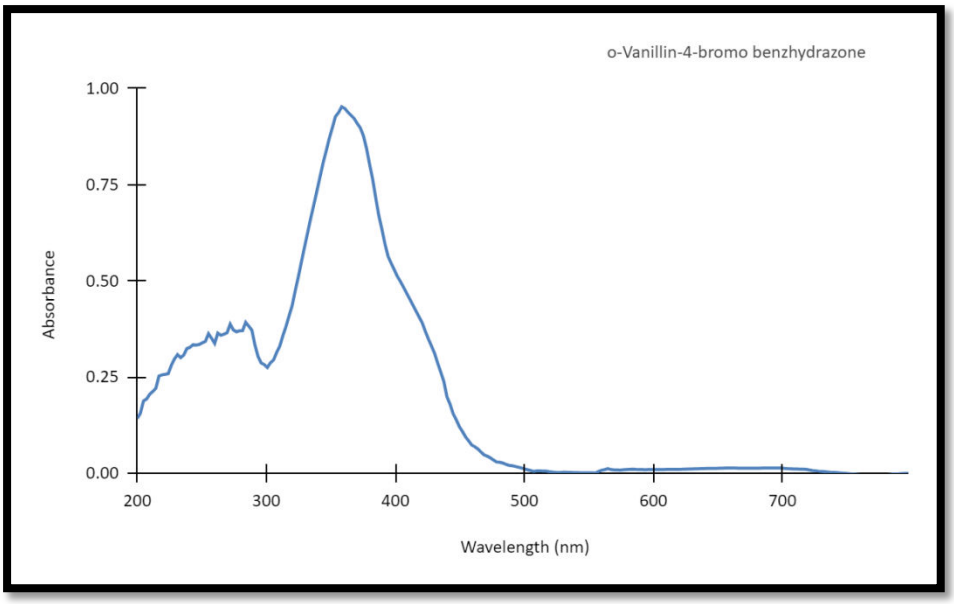

Fig. S12. UV-Vis spectrum of o-Vanillin-4-bromo benzhydrazone

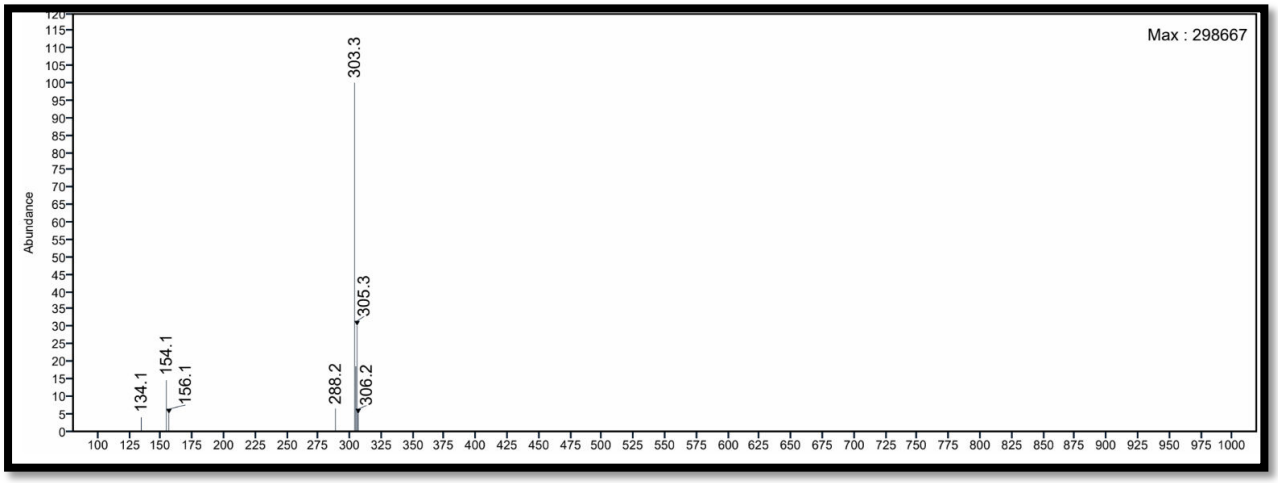

Fig. S13. Mass spectrum of o-Vanillin-4-chloro benzhydrazone

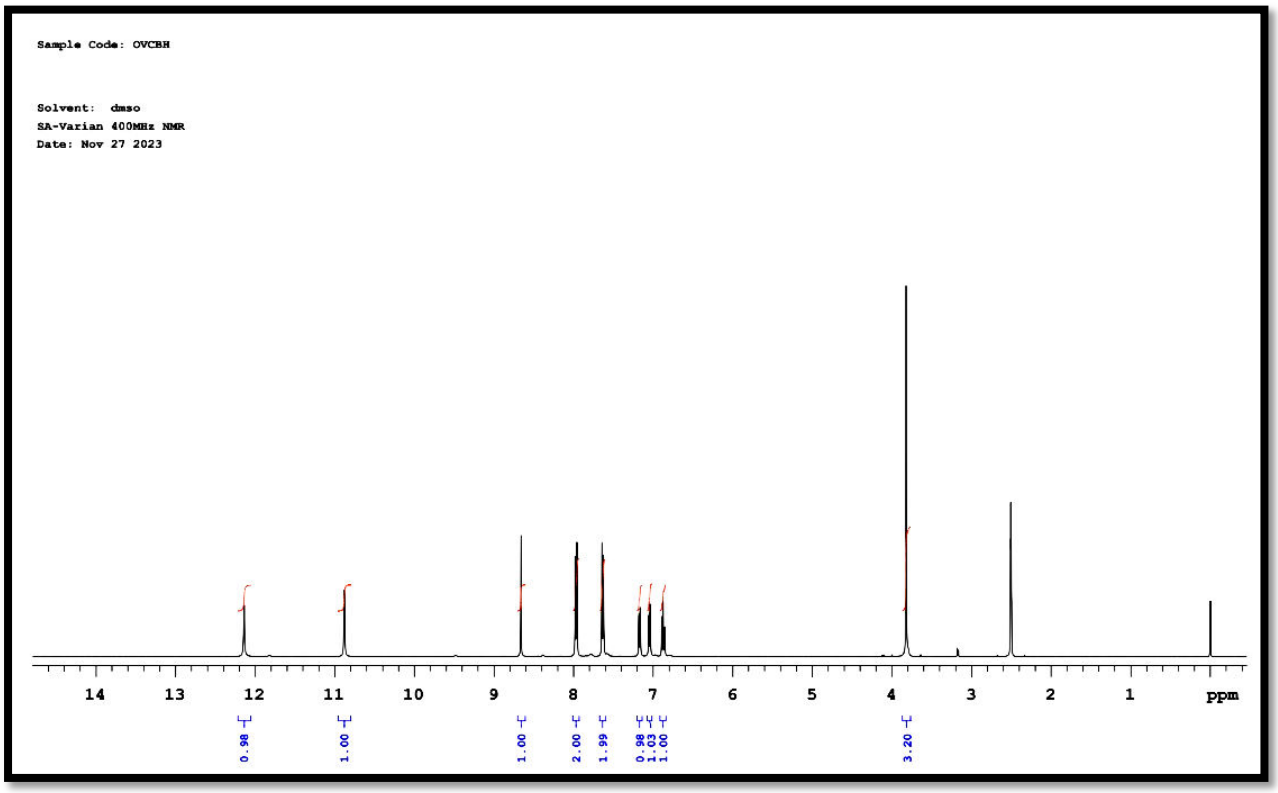

Fig. S14. 1H NMR spectrum of o-Vanillin-4-chloro benzhydrazone

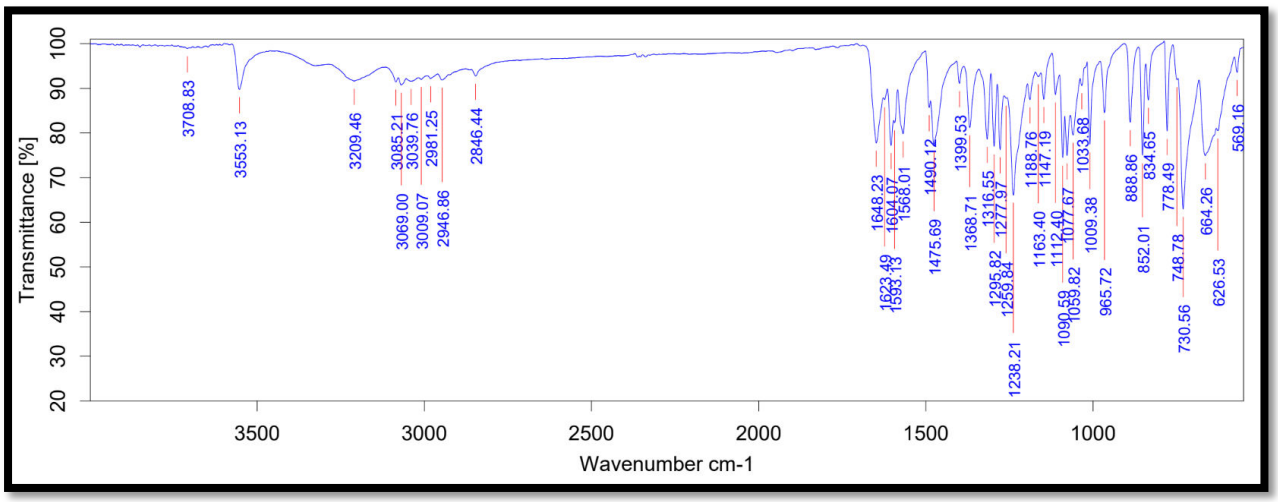

Fig. S15. IR spectrum of o-Vanillin-4-chloro benzhydrazone

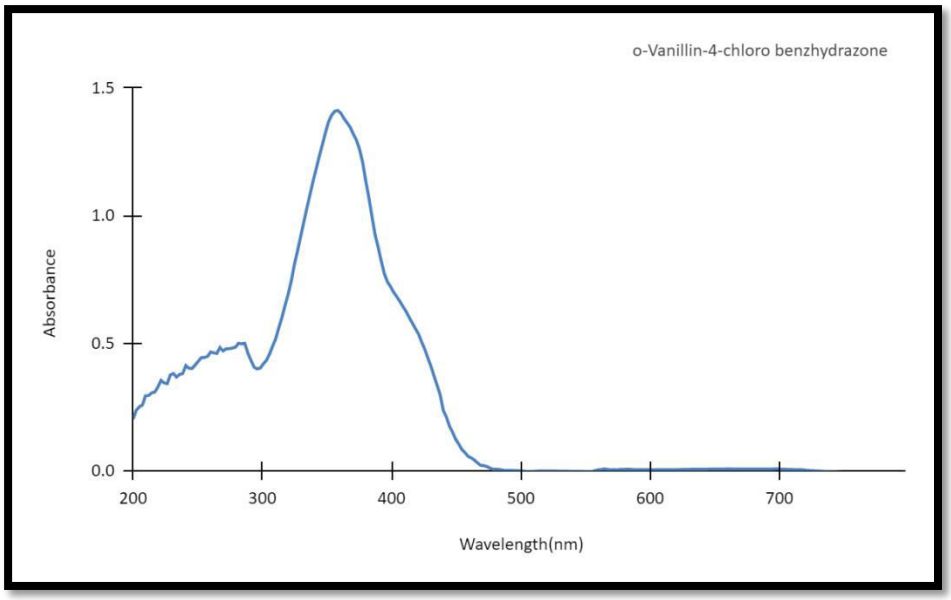

Fig. S16. UV-Vis spectrum of o-Vanillin-4-chloro benzhydrazone

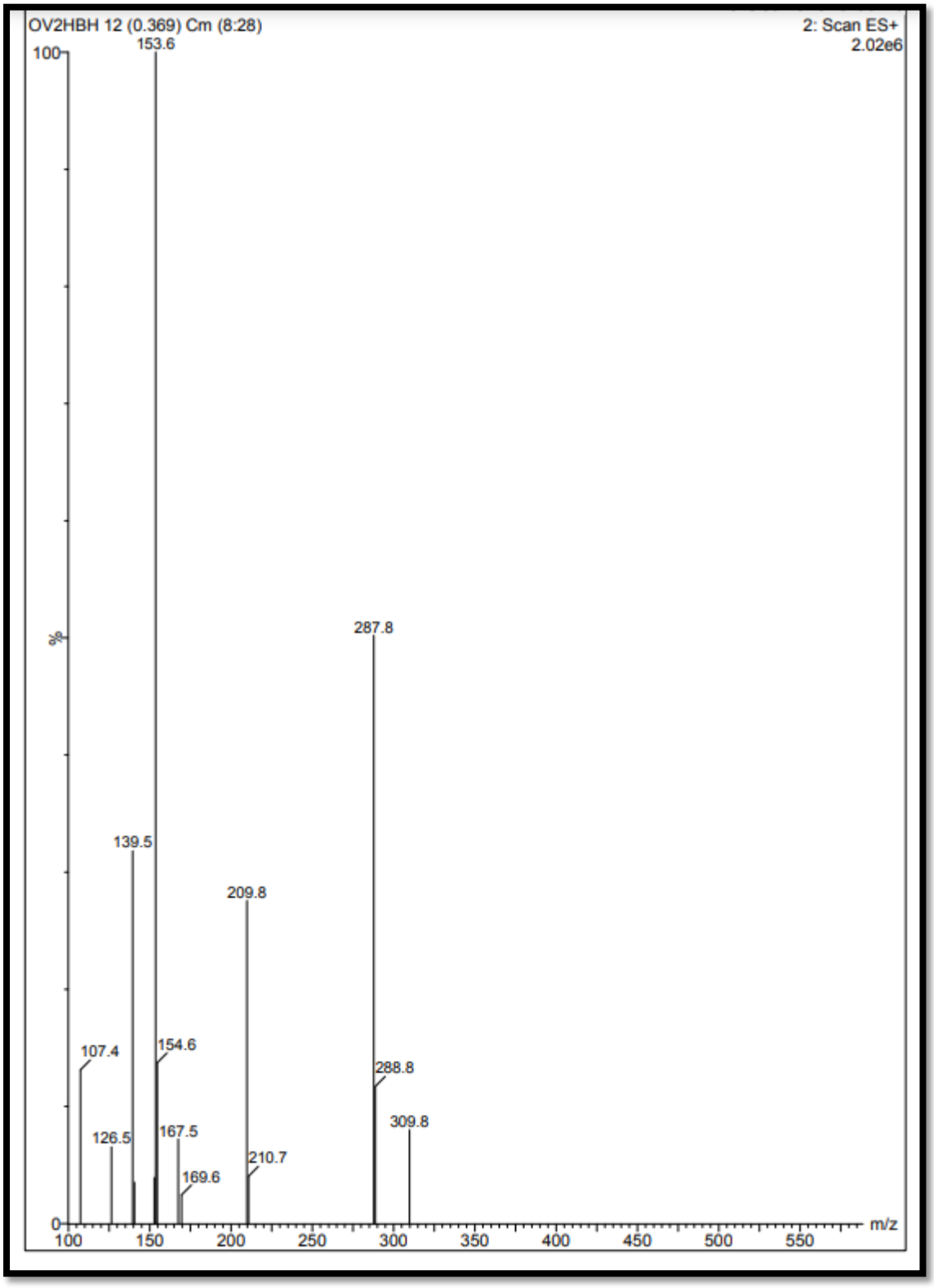

Fig. S17. Mass spectrum of o-Vanillin-2-hydroxy benzhydrazone

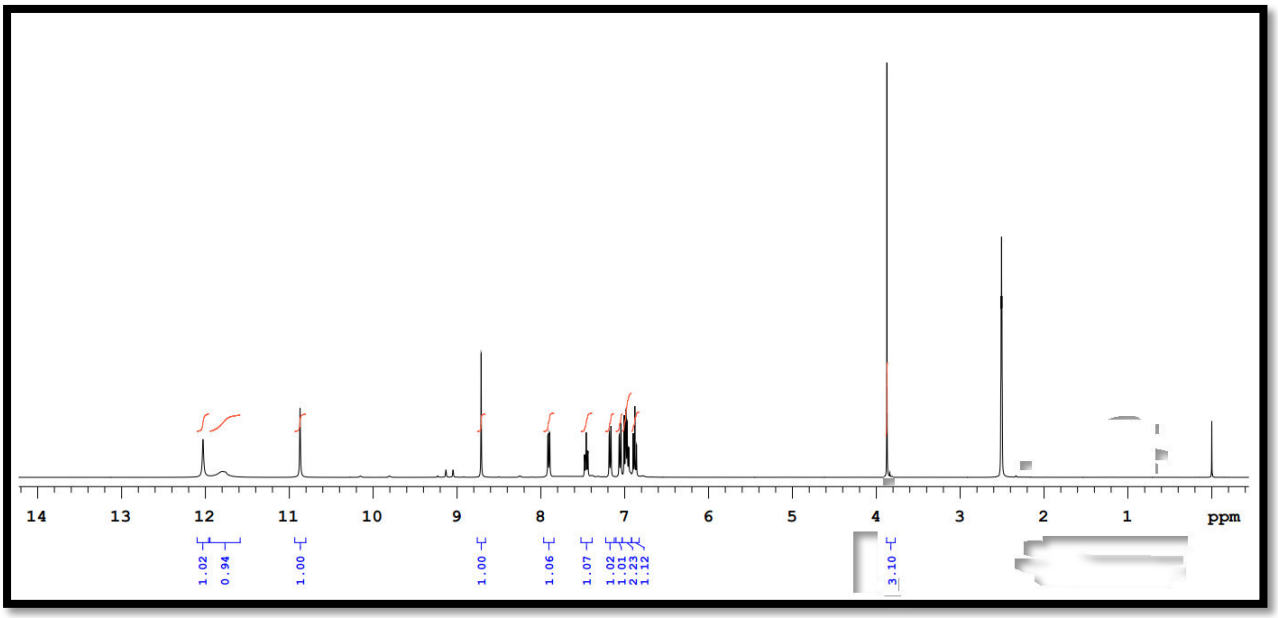

Fig. S18. 1H NMR spectrum of o-Vanillin-2-hydroxy benzhydrazone

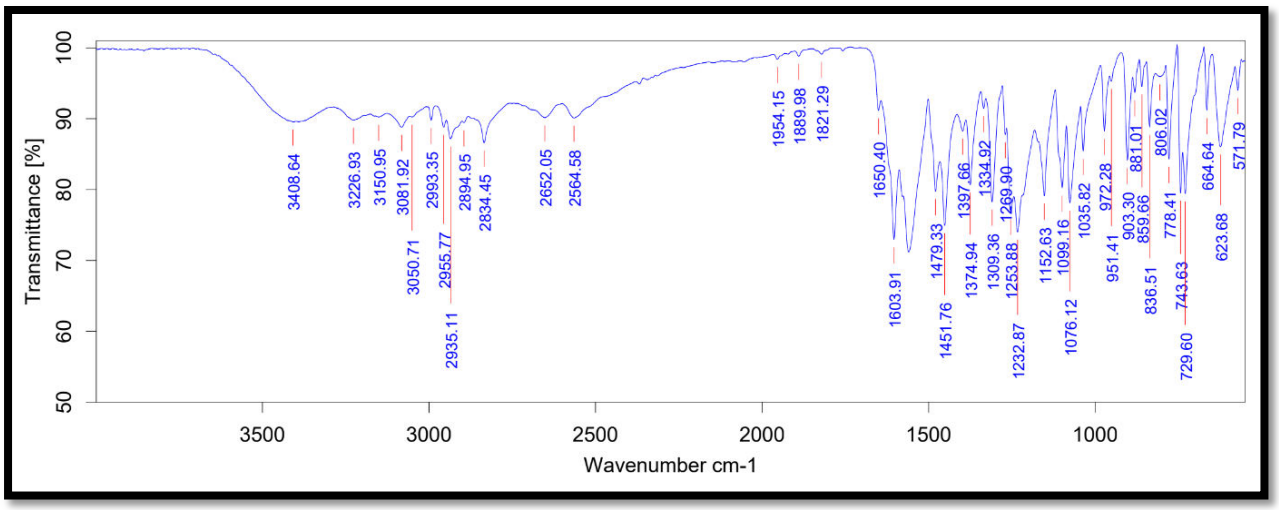

Fig. S19. IR spectrum of o-Vanillin-2-hydroxy benzhydrazone

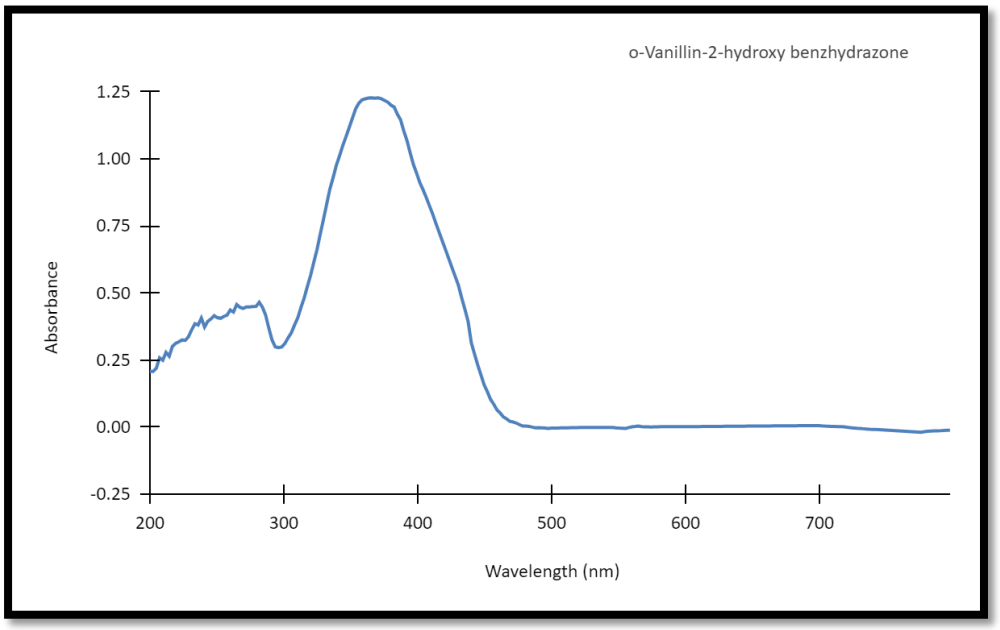

Fig. S20. UV-Vis spectrum of o-Vanillin-2-hydroxy benzhydrazone

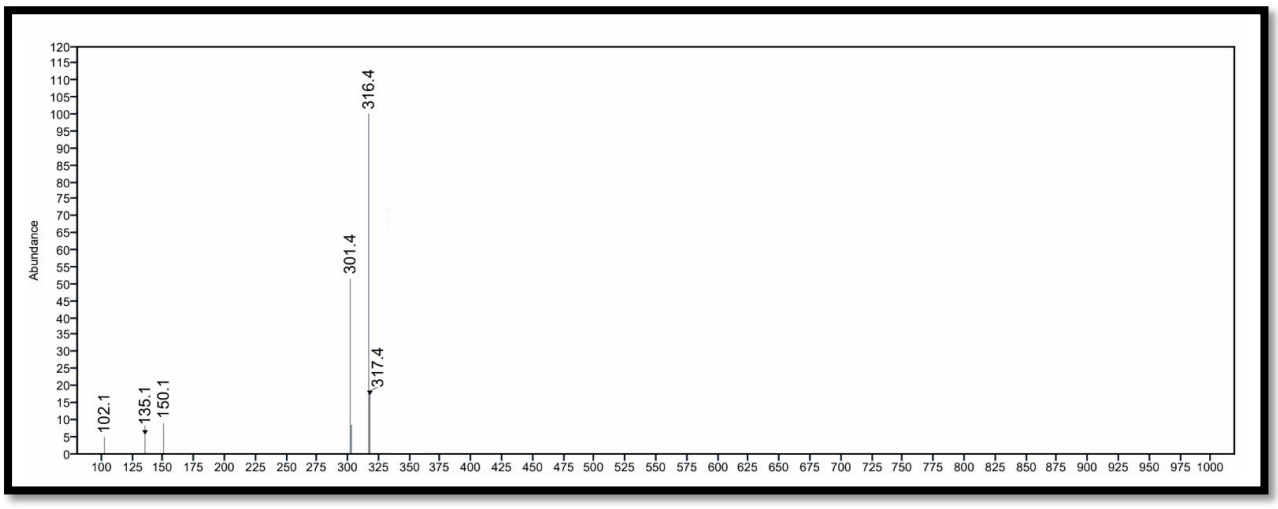

Fig. S21. Mass spectrum of o-Vanillin-3-nitro benzhydrazone

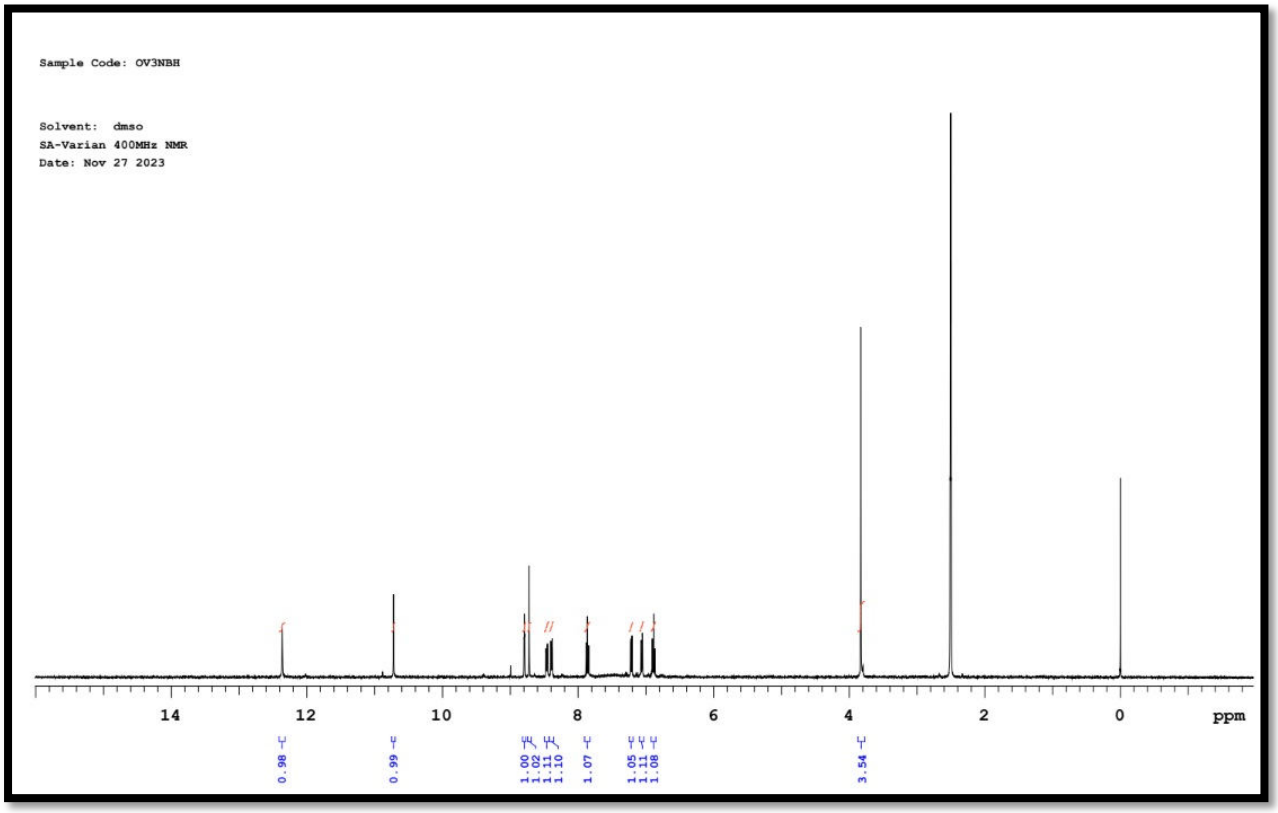

Fig. S22. 1H NMR spectrum of o-Vanillin-3-nitro benzhydrazone

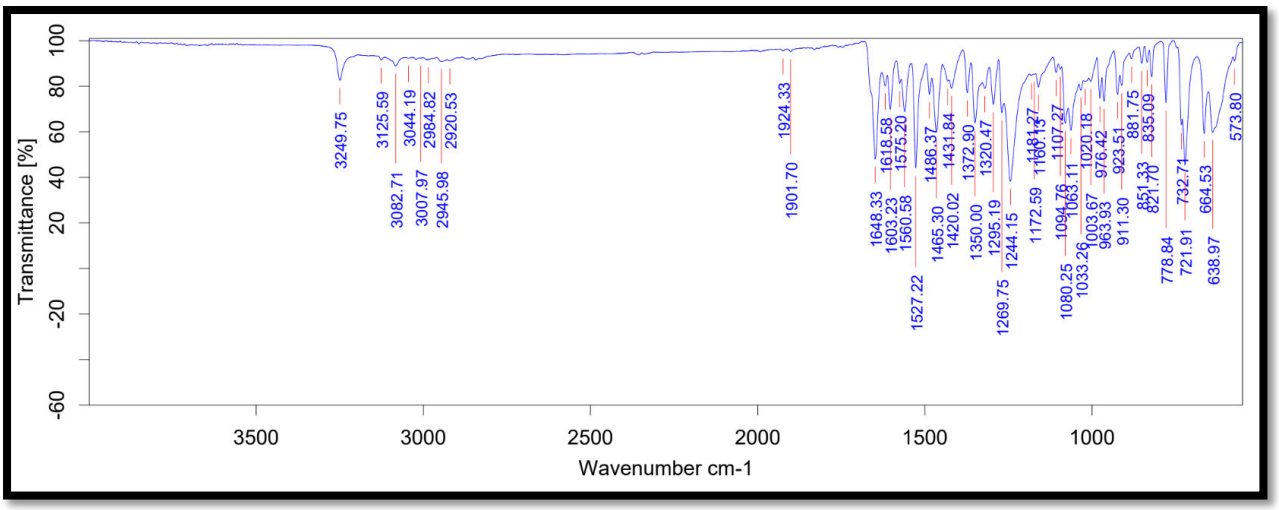

Fig. S23. IR spectrum of o-Vanillin-3-nitro benzhydrazone

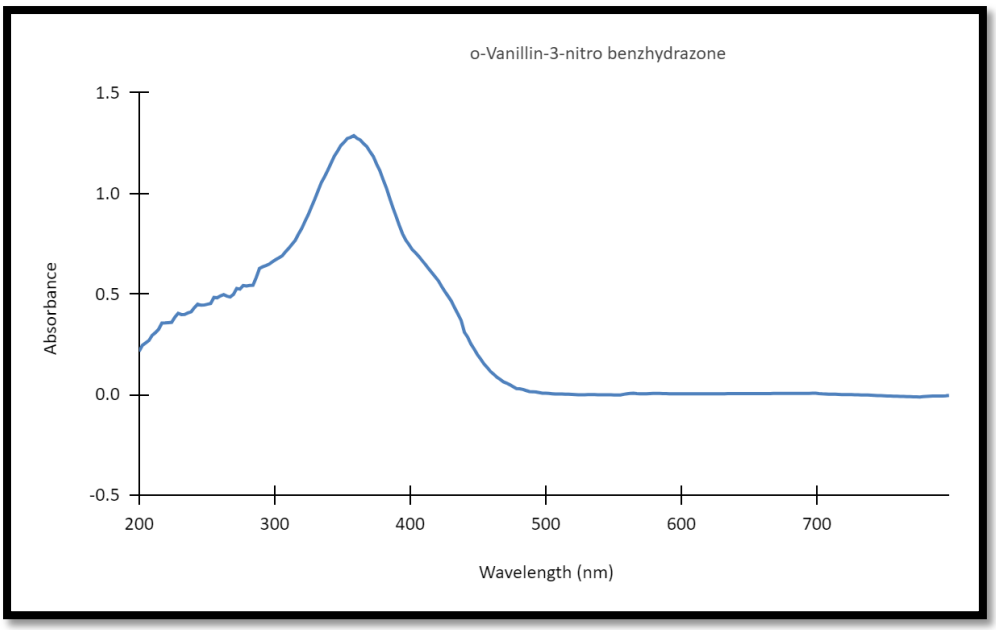

Fig. S24. UV-Vis spectrum of o-Vanillin-3-nitro benzhydrazone

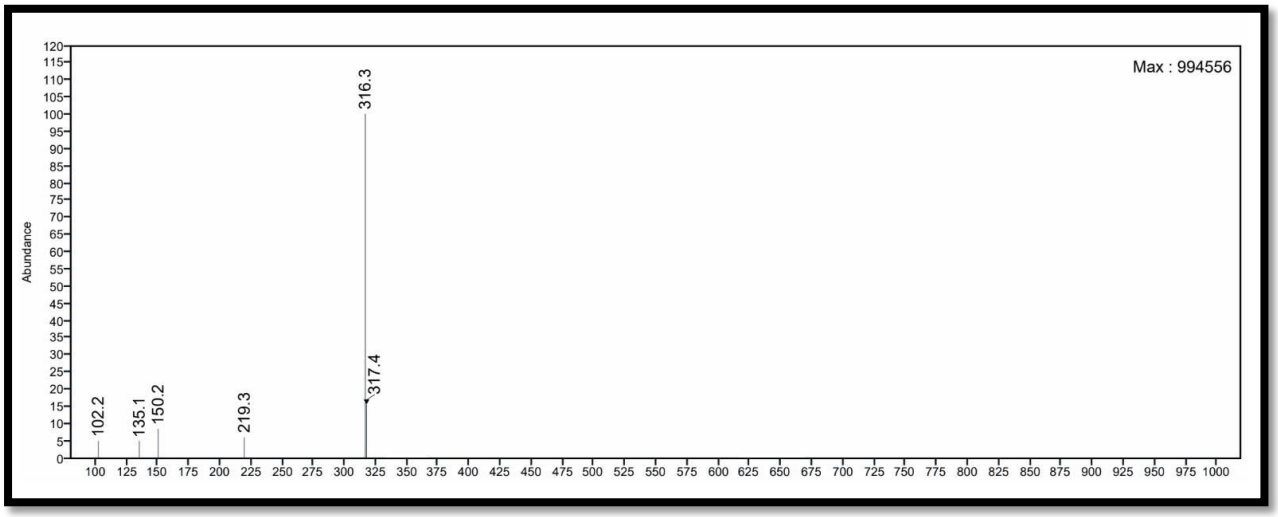

Fig. S25. Mass spectrum of o-Vanillin-4-nitro benzhydrazone

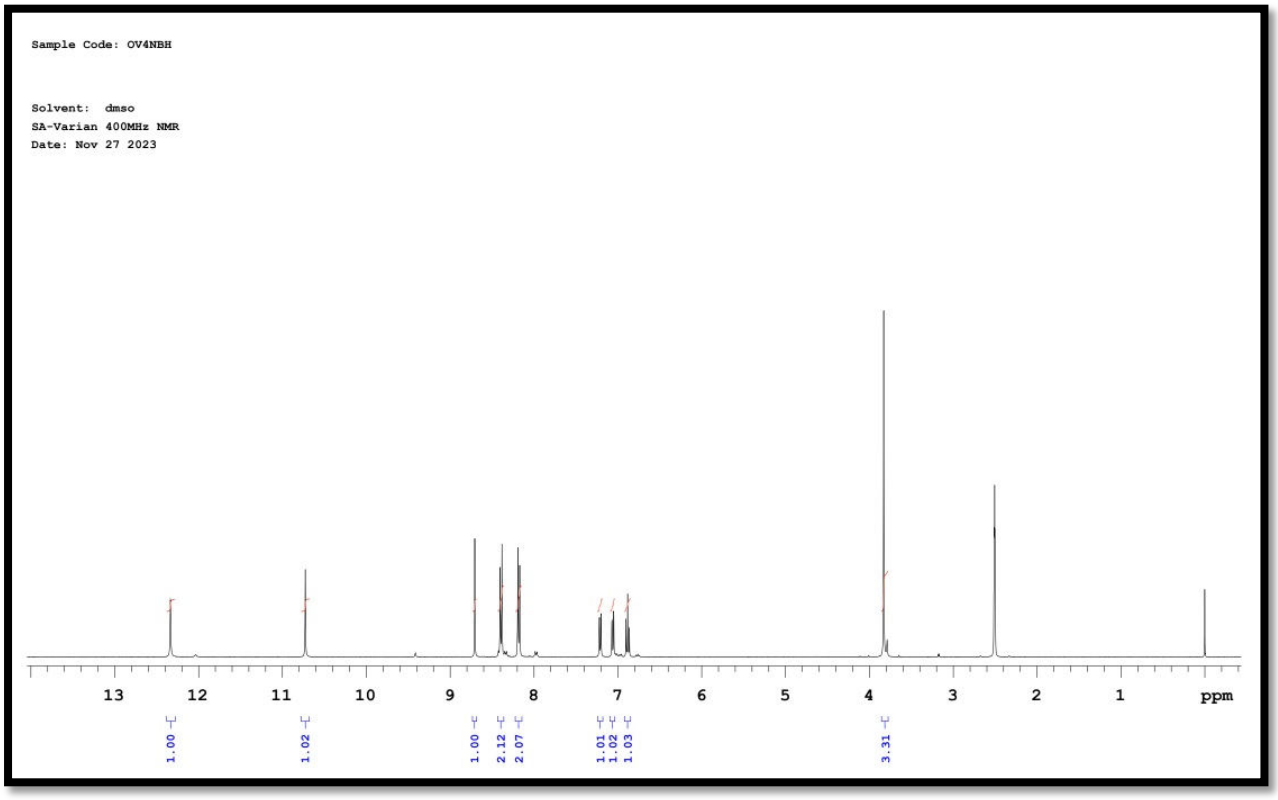

Fig. S26. 1H NMR spectrum of o-Vanillin-4-nitro benzhydrazone

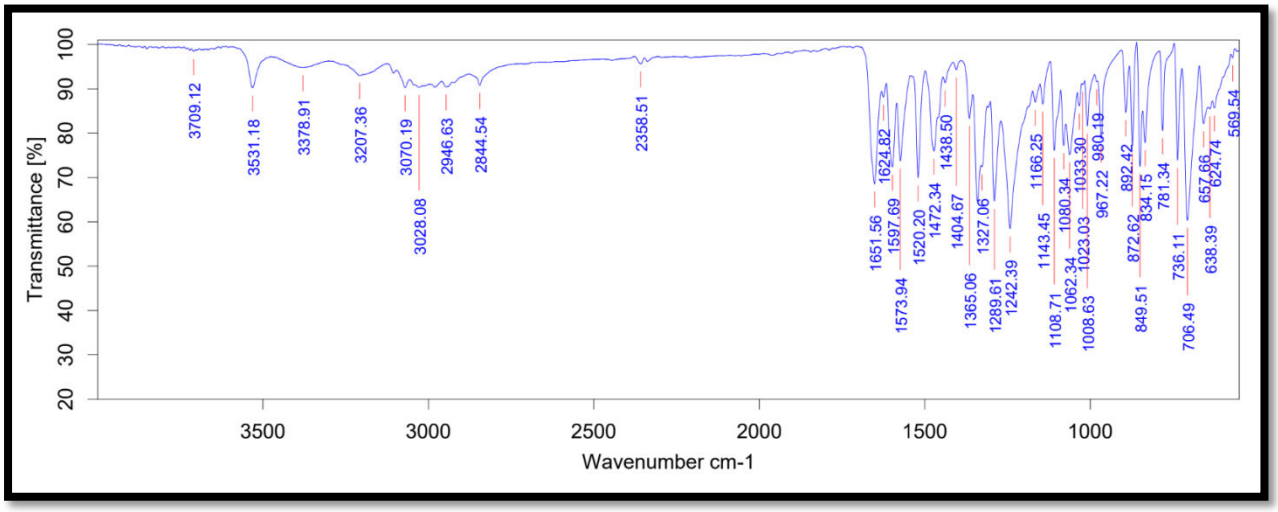

Fig. S27. IR spectrum of o-Vanillin-4-nitro benzhydrazone

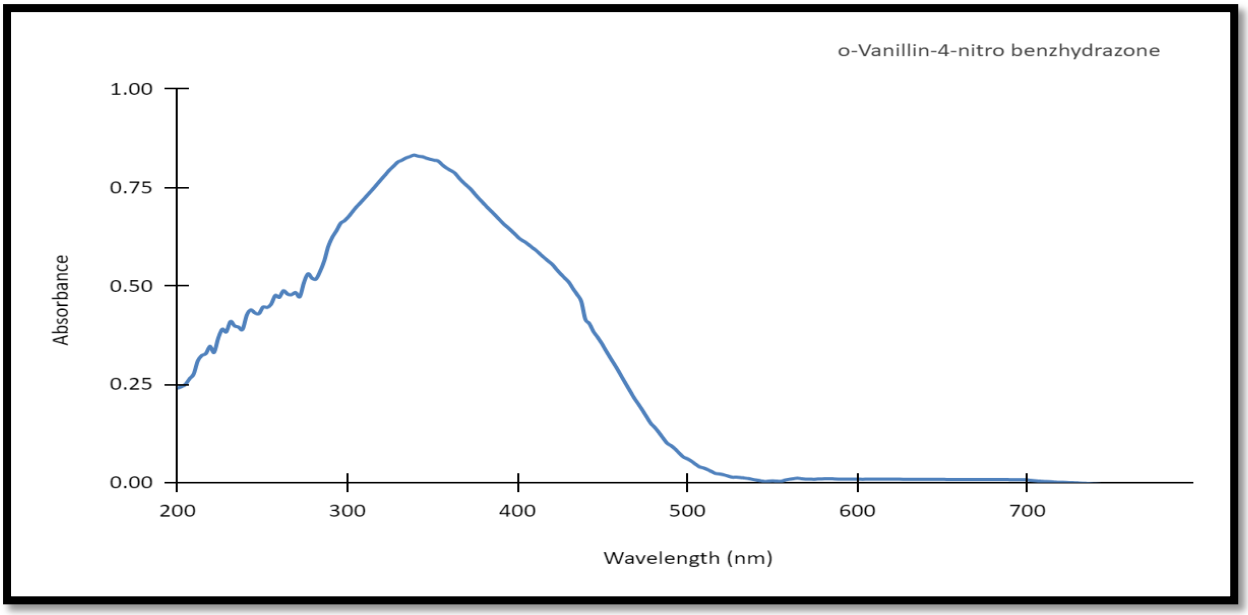

Fig. S28. UV-Vis spectrum of o-Vanillin-4-nitro benzhydrazone

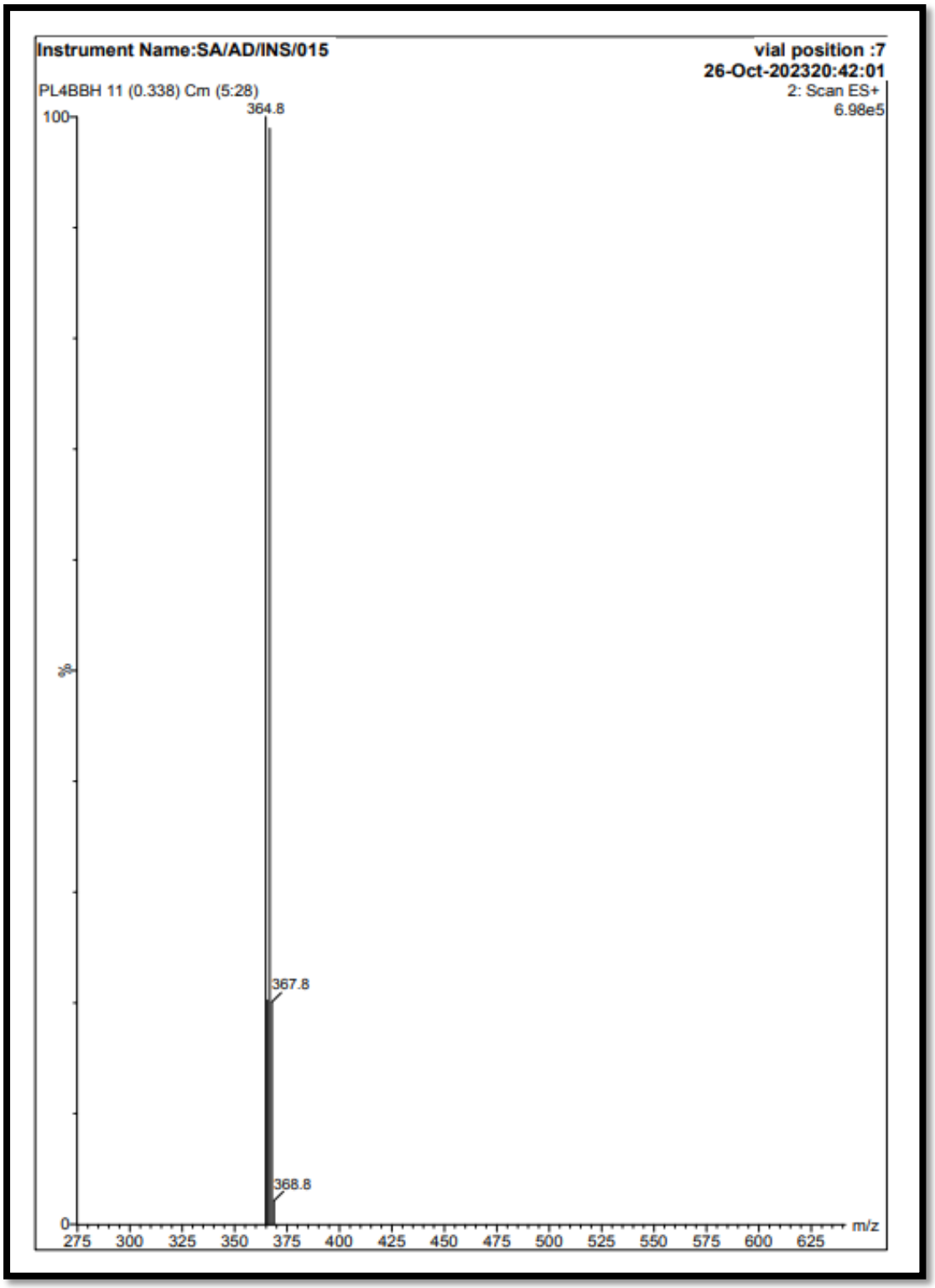

.

Fig. S29. Mass spectrum of Pyridoxal-4-bromo benzhydrazone

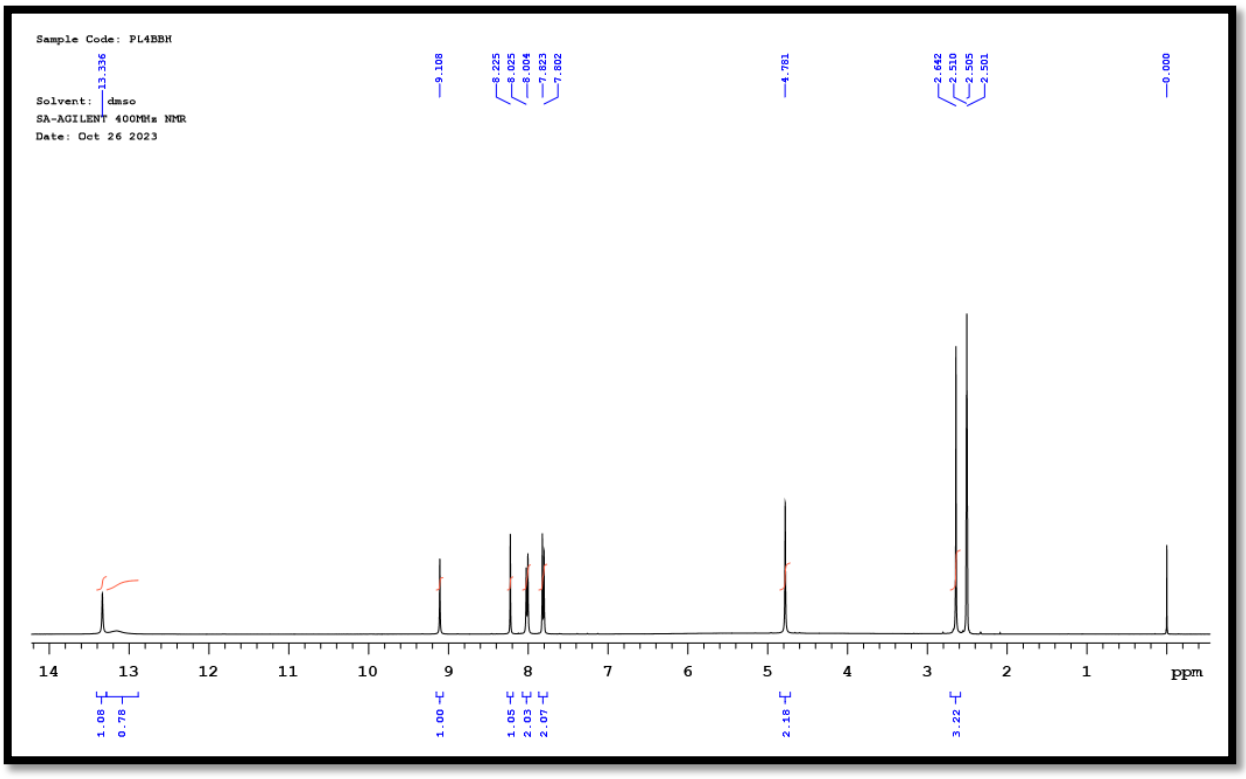

Fig. S30. 1H NMR spectrum of Pyridoxal-4-bromo benzhydrazone

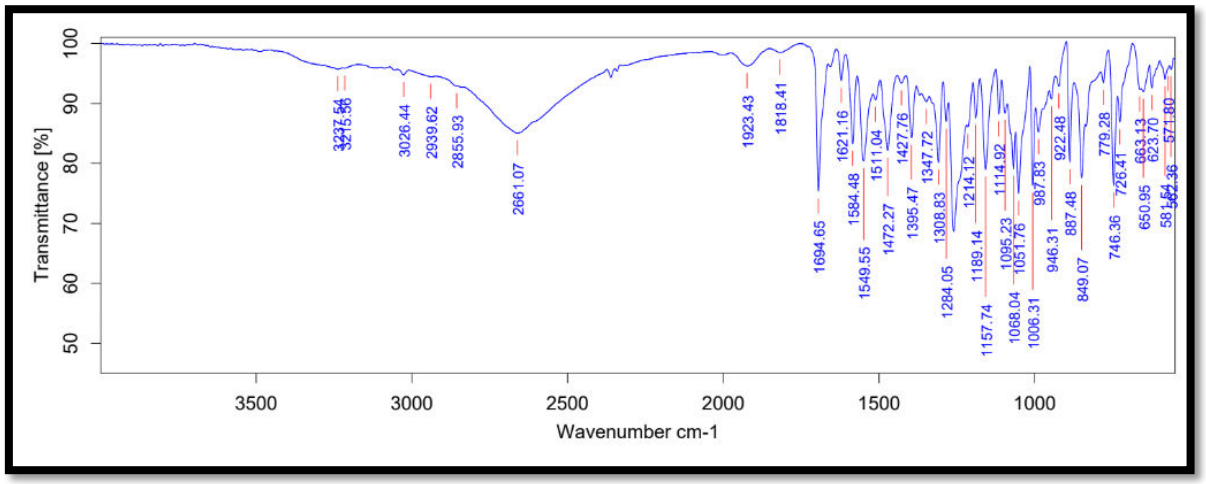

Fig. S31. IR spectrum of Pyridoxal-4-bromo benzhydrazone

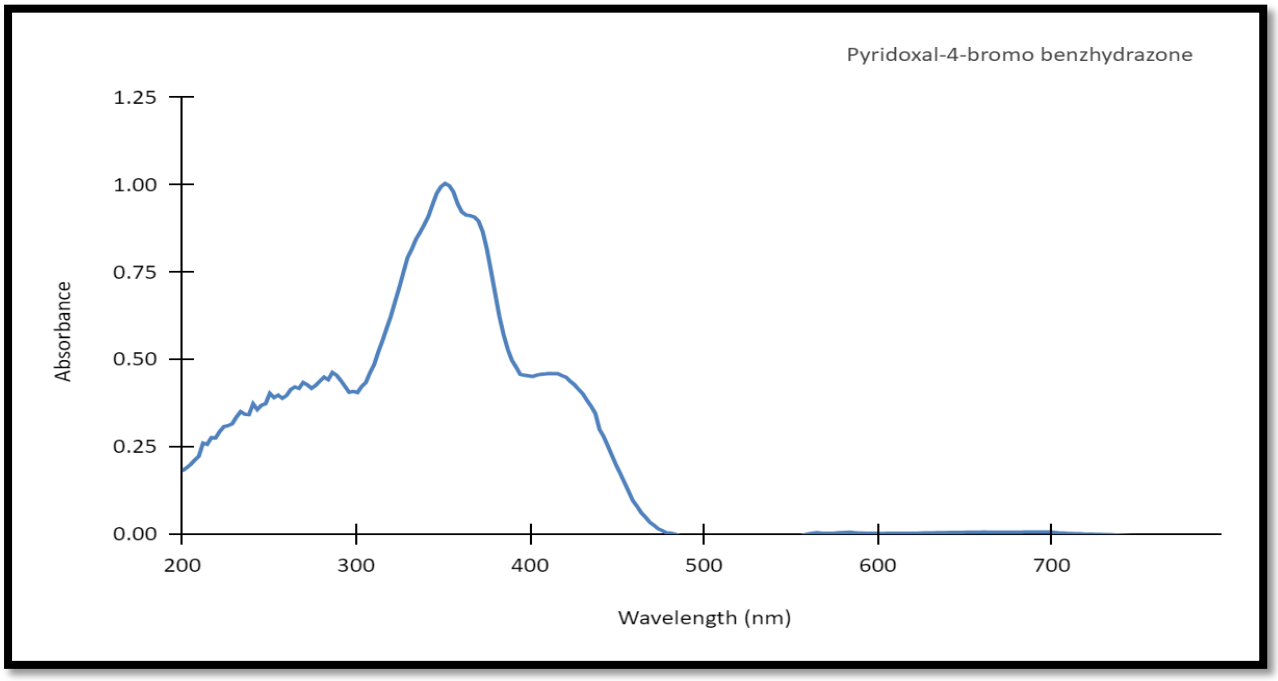

Fig. S32. UV-Vis spectrum of Pyridoxal-4-bromo benzhydrazone

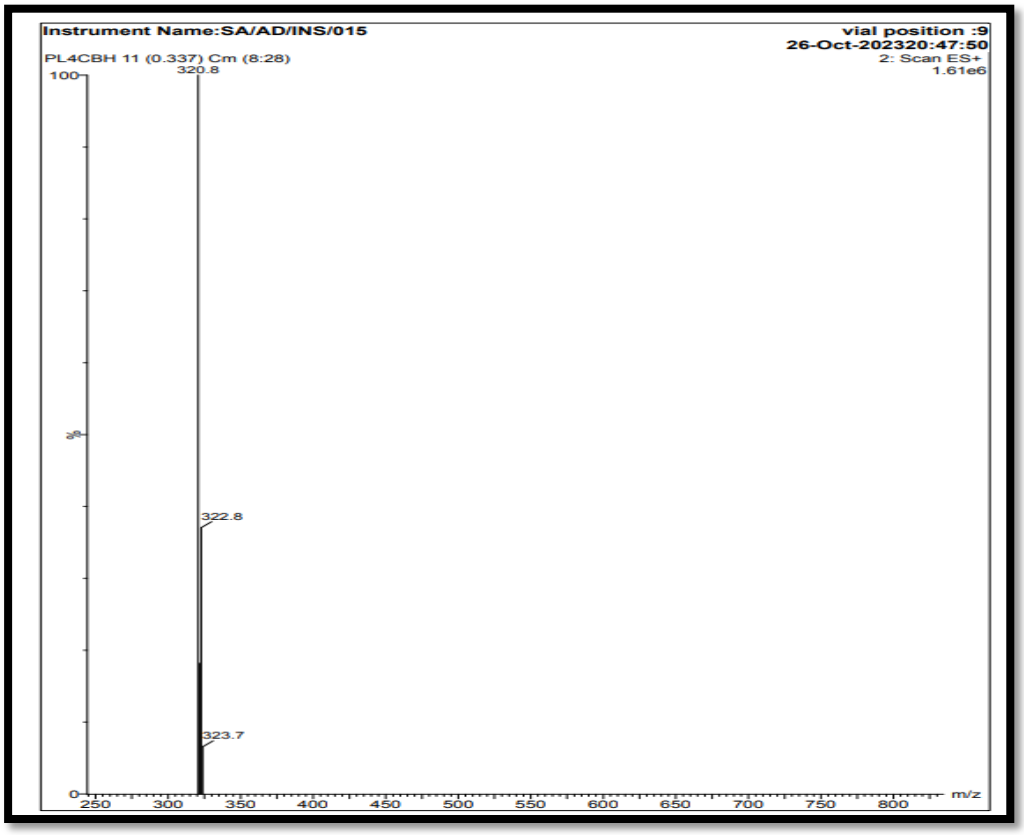

Fig. S33. Mass spectrum of Pyridoxal-4-chloro benzhydrazone

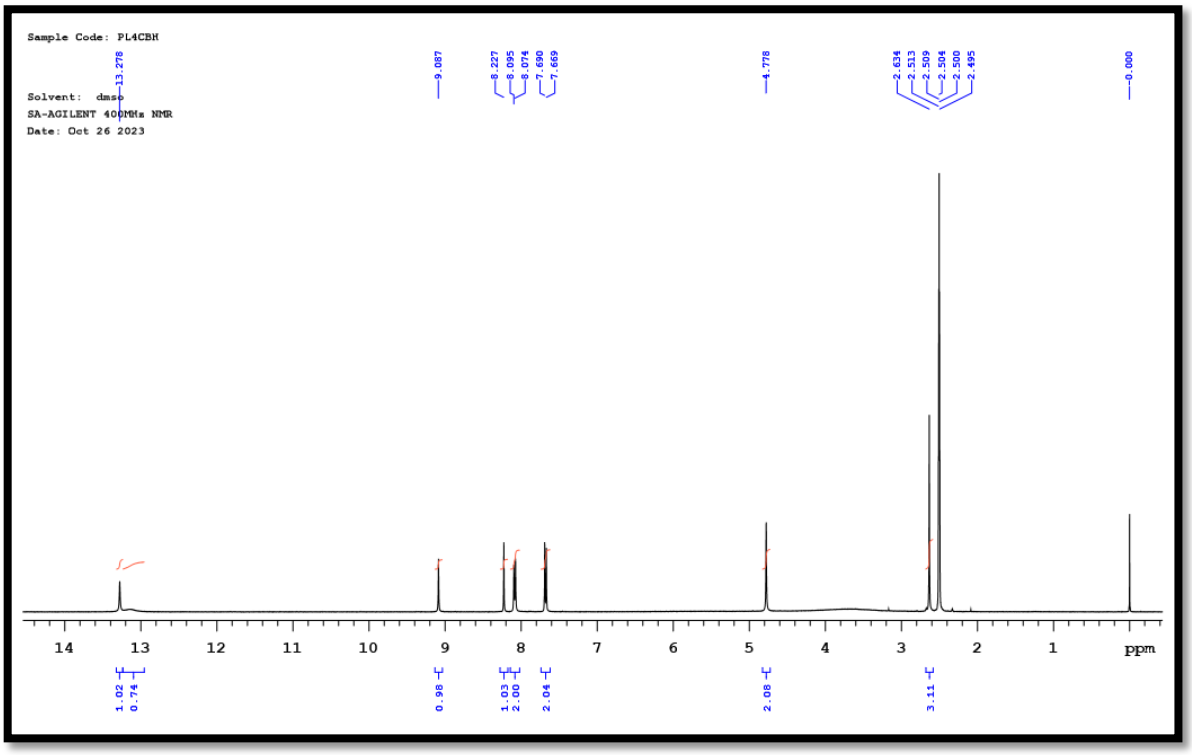

Fig. S34. 1H NMR spectrum of Pyridoxal-4-chloro benzhydrazone

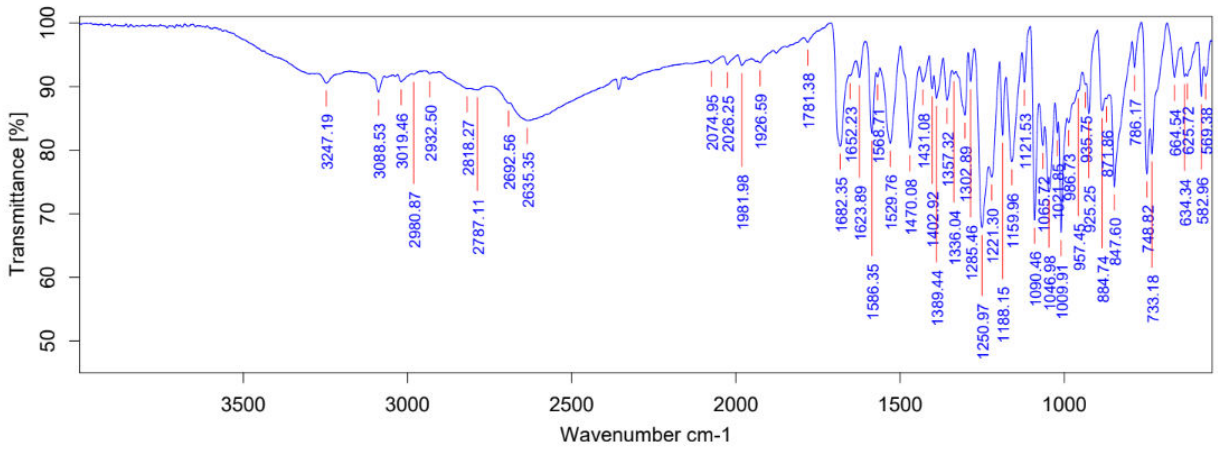

Fig. S35. IR spectrum of Pyridoxal-4-chloro benzhydrazone

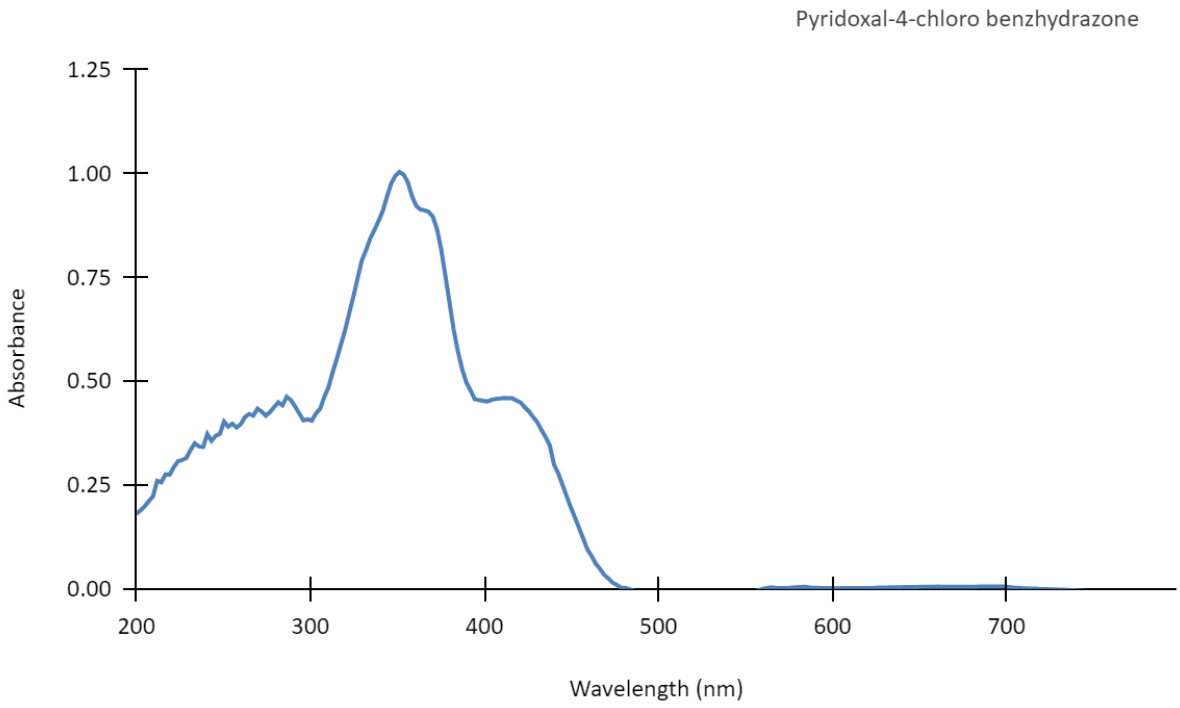

Fig. S36. UV-Vis spectrum of Pyridoxal-4-chloro benzhydrazone

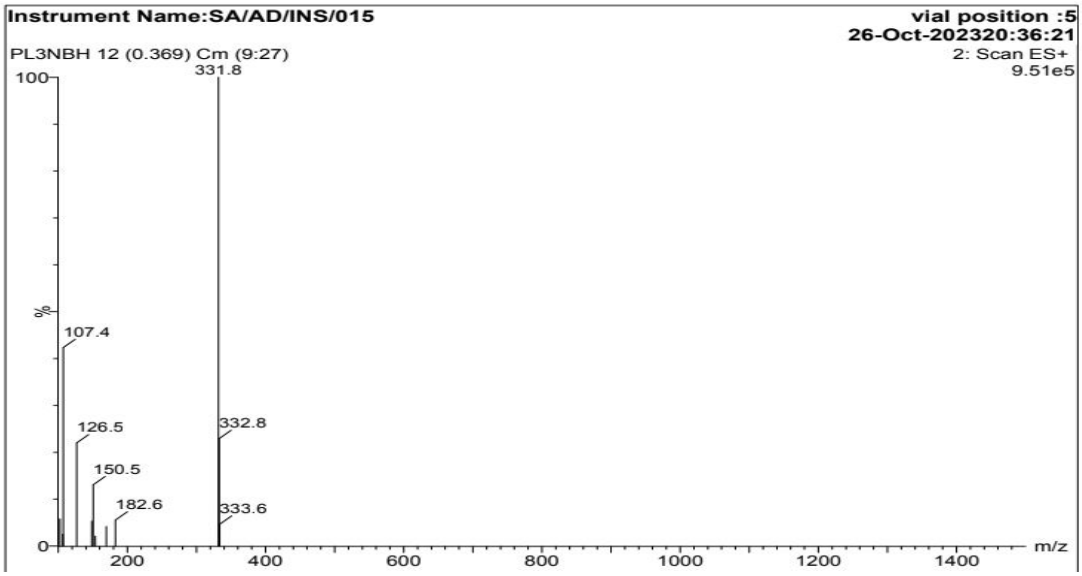

Fig. S37. Mass spectrum of Pyridoxal-3-nitro benzhydrazone

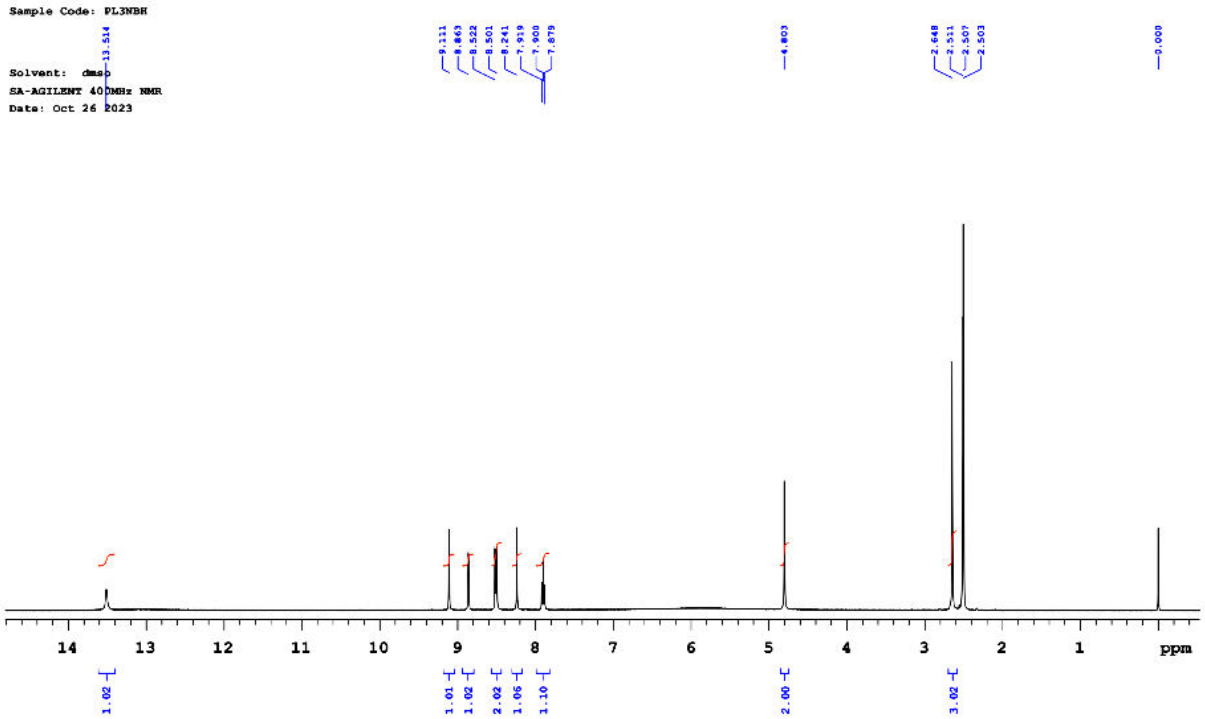

Fig. S38. 1H NMR spectrum of Pyridoxal-3-nitro benzhydrazone

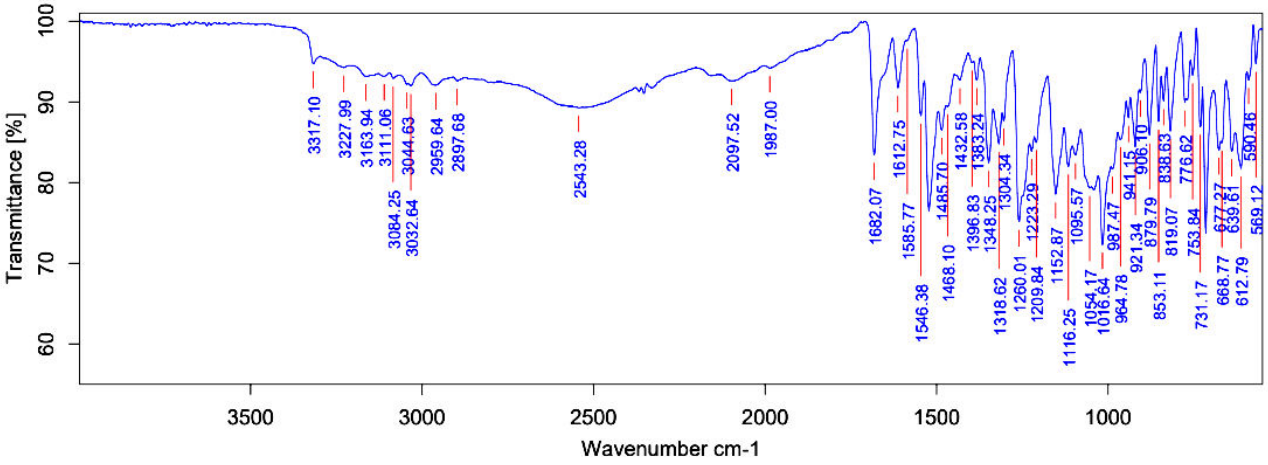

Fig. S39. IR spectrum of Pyridoxal-3-nitro benzhydrazone

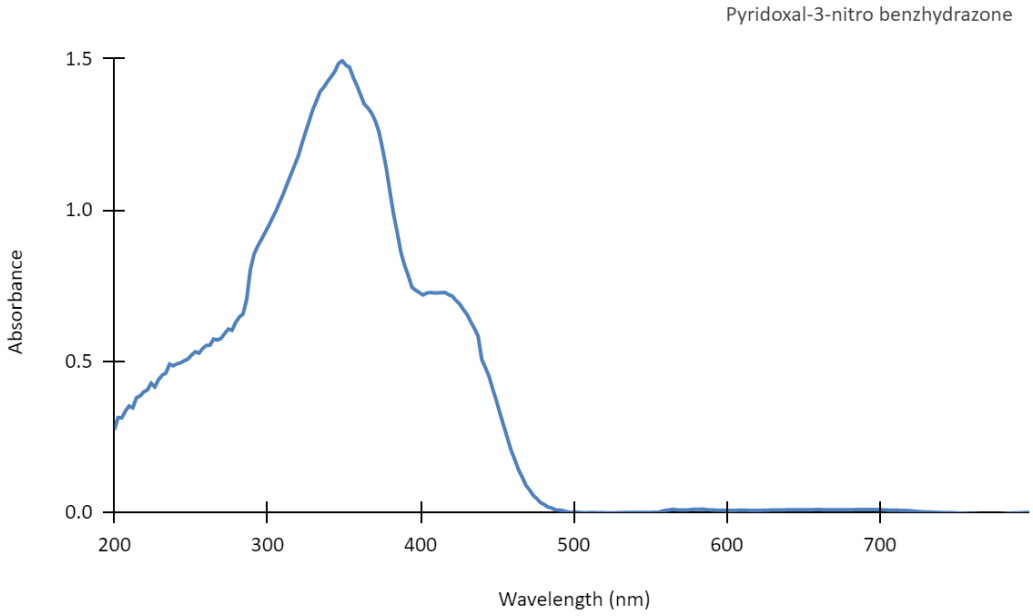

Fig. S40. UV-Vis spectrum of Pyridoxal-3-nitro benzhydrazone

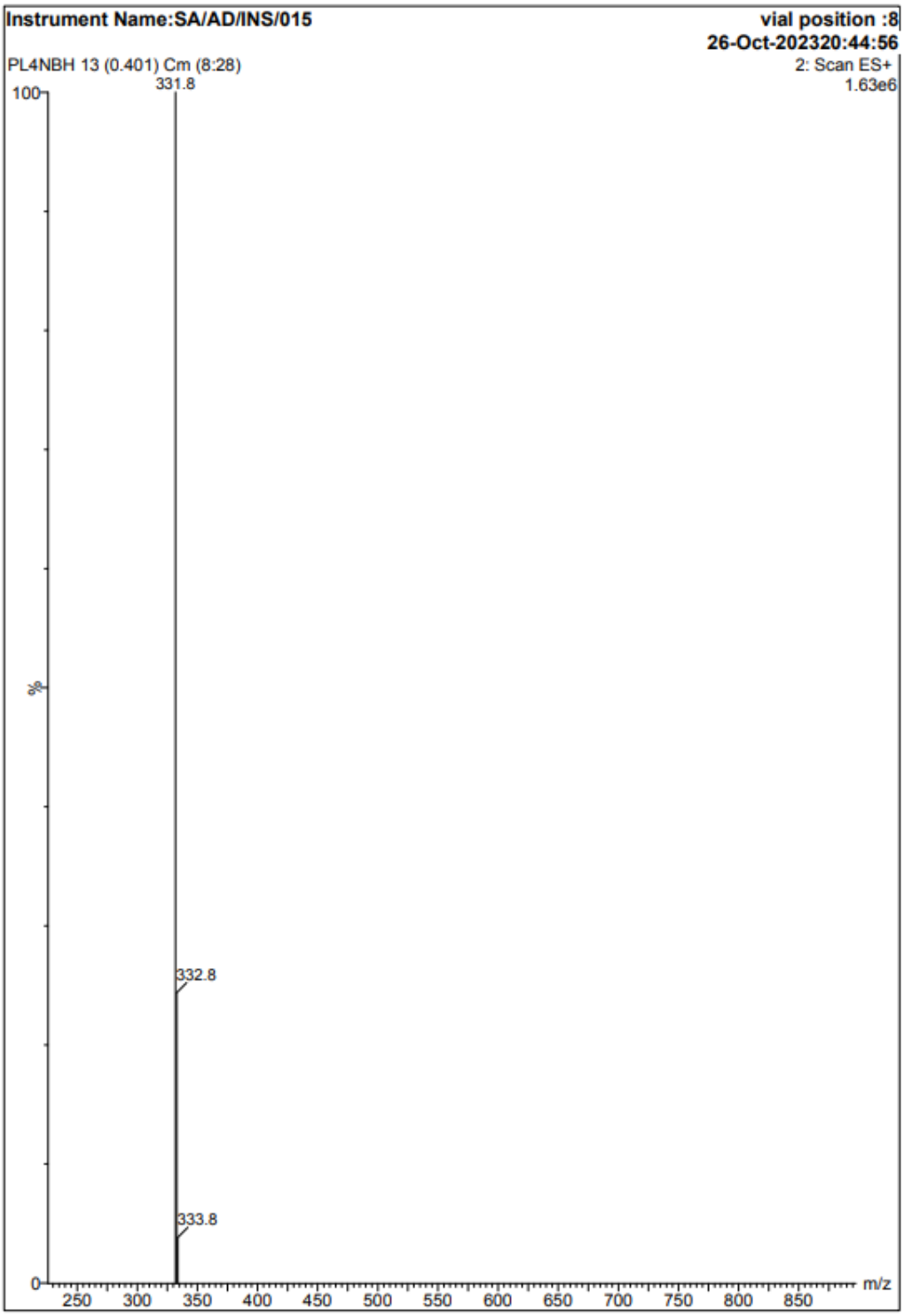

Fig. S41. Mass spectrum of Pyridoxal-4-nitro benzhydrazone

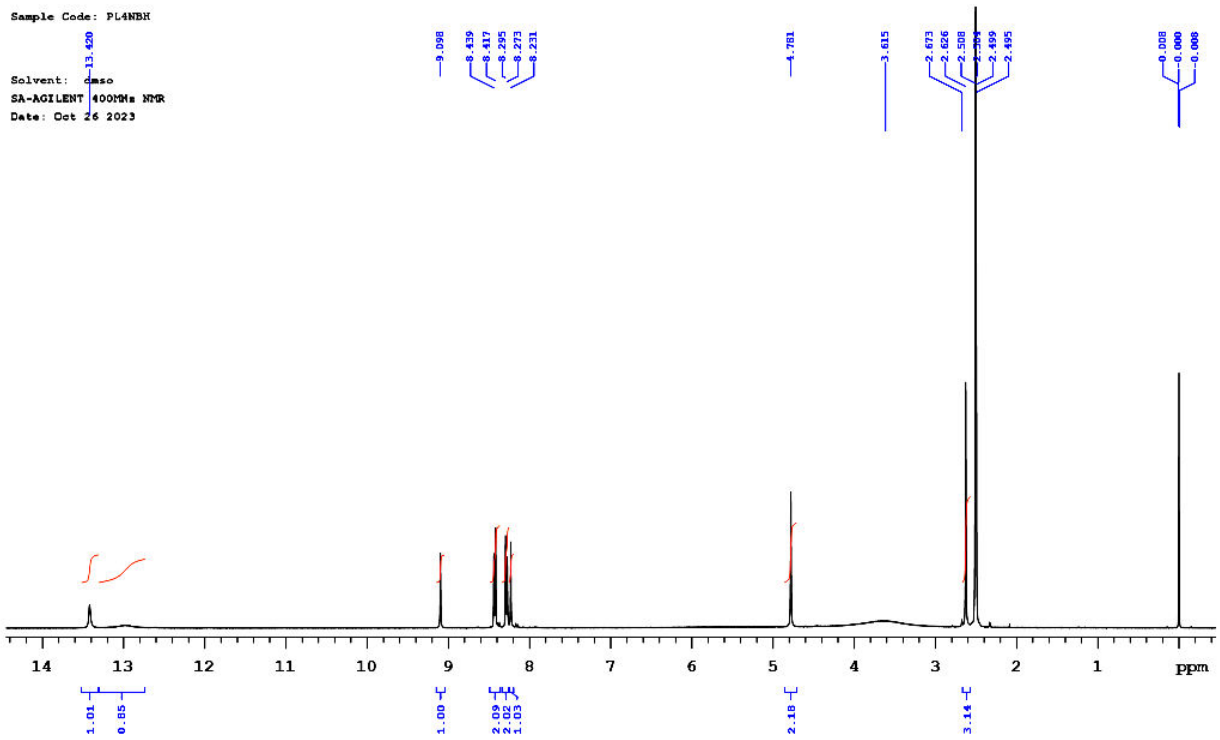

Fig. S42. 1H NMR spectrum of Pyridoxal-4-nitro benzhydrazone

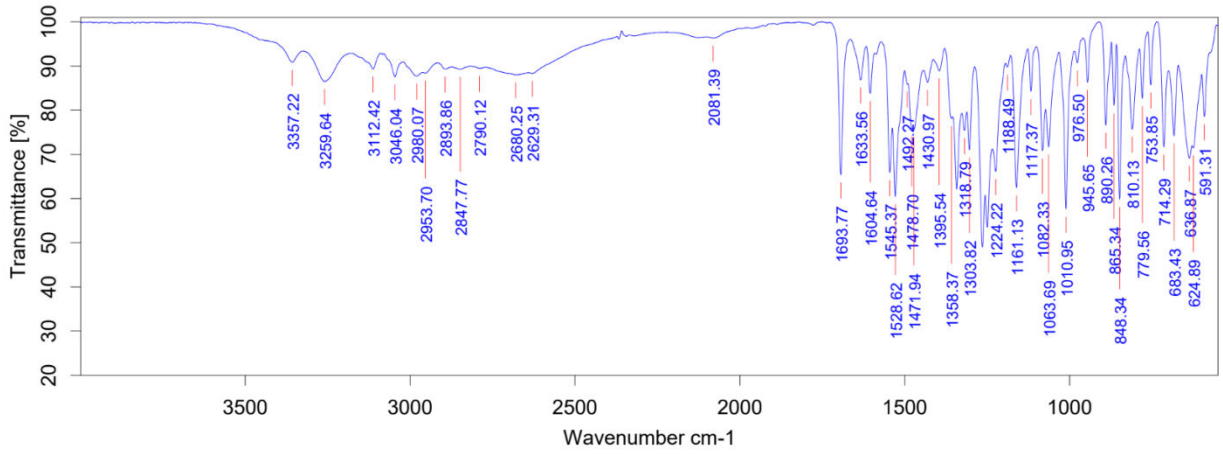

Fig. S43. IR spectrum of Pyridoxal-4-nitro benzhydrazone

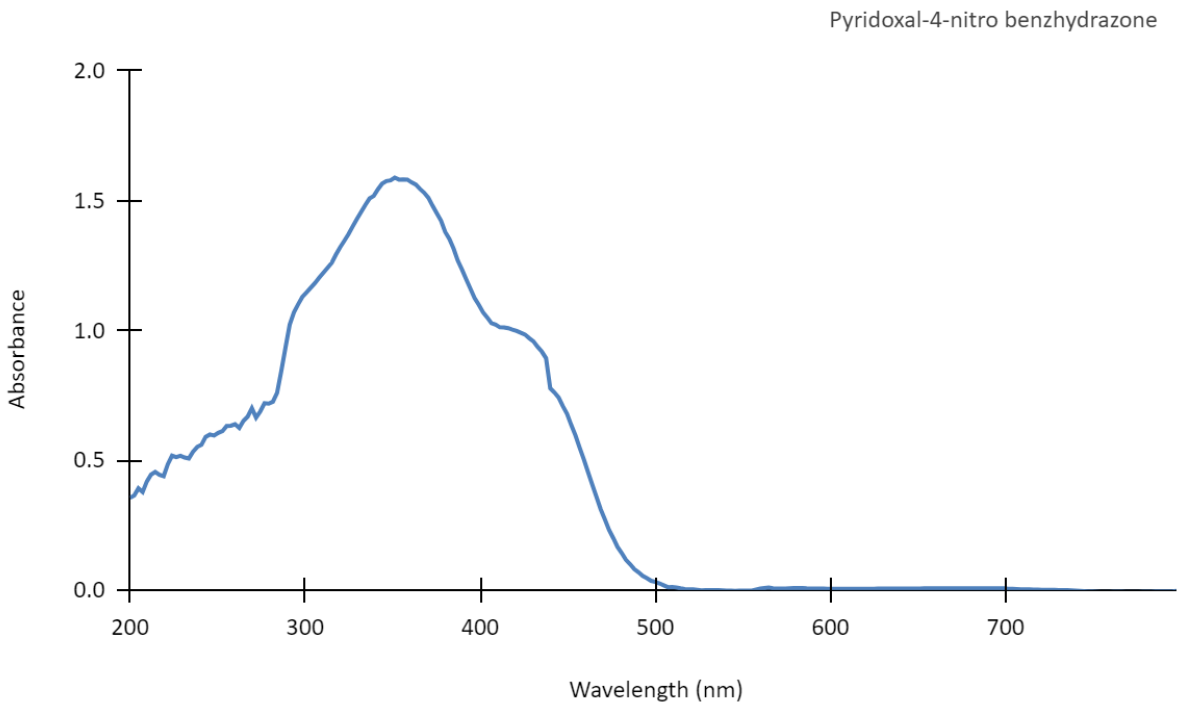

Fig. S44. UV-Vis spectrum of Pyridoxal-4-nitro benzhydrazone